© 2018. Published by The Company of Biologists Ltd | Development (2018) 145, dev168716. doi:10.1242/dev.168716

STEM CELLS AND REGENERATION

RESEARCH ARTICLE

Wingless promotes EGFR signaling in follicle stem cells to maintain self-renewal

Rebecca P. Kim-Yip and Todd G. Nystul*

ABSTRACT

Adult stem cell niche boundaries must be precisely maintained to facilitate the segregation of stem cell and daughter cell fates. However, the mechanisms that govern this process in epithelial tissues are not fully understood. In this study, we investigated the relationship between two signals, Wnt and EGFR, that are necessary for self-renewal of the epithelial follicle stem cells (FSCs) in the *Drosophila* ovary, but must be downregulated in cells that have exited the niche to allow for differentiation. We found that Wingless produced by inner germarial sheath (IGS) cells acts over a short distance to activate Wnt signaling in FSCs, and that movement across the FSC niche boundary is limited. In addition, we show that Wnt signaling functions genetically upstream of EGFR signaling by activating the expression of the EGFR ligand, Spitz, and that constitutive activation of EGFR partially rescues the self-renewal defect caused by loss of Wnt signaling. Collectively, our findings support a model in which the Wnt and EGFR pathways operate in a signaling hierarchy to promote FSC self-renewal.

KEY WORDS: Epithelial stem cell, *Drosophila*, Ovary, Wnt, EGFR, Niche

INTRODUCTION

Adult epithelial stem cells divide to produce differentiated progeny that replace lost or damaged cells in the tissue, or self-renewing progeny to replenish the population of stem cells. This asymmetry of cell fates is enforced by the adult stem cell niche microenvironment, which is essential for maintenance and self-renewal of the cell within that environment, ensuring that a consistent population of stem cells is available for regeneration of differentiated daughter cells. The mechanisms by which these signaling ligands are communicated between niche and epithelial stem cells with specificity, as well as how they maintain self-renewal robustly, are not fully understood.

The follicle epithelium of the *Drosophila* ovary is a tractable model that can be genetically manipulated to study epithelial stem cells in their native tissue environment (Sahai-Hernandez et al., 2012). The *Drosophila* ovary is composed of long strands of developing follicles, called ovarioles, and oogenesis begins at the anterior tip of each ovariole in a structure called the germarium. The germarium is divided into four regions (Regions 1, 2a, 2b and 3) that correspond to distinct stages of germ cell development (Fig. 1A). In Region 1, two somatic cell types, the cap cells and terminal filament cells, provide cues that regulate the proliferation and self-renewal of germline stem cells (GSCs) (Chen et al., 2011). GSC divisions produce cystoblasts that undergo four rounds of division with incomplete cytokinesis as they move downstream through the germarium to become 16-cell germline cysts. At this stage, referred to as Region 2a, two clearly identifiable 16-cell cysts are arranged side by side across the width of the germarium. In Regions 1 and 2a, the germ cells are surrounded by a population of somatic inner germarial sheath cells (IGS cells, also referred to as escort cells) that wrap around each cyst with long cytoplasmic processes and provide important germ cell differentiation cues. As germ cell cysts move from Region 2a to 2b, they shed the IGS cell layer, widen to span the entire width of the germarium, and become encapsulated by the follicle cells. Next, as the germ cell cyst moves further downstream into Region 3, it becomes more circular and the follicle cells organize into a single-layered epithelium. Many studies have confirmed the existence of follicle stem cells (FSCs) at the Region 2a/2b border (Chang et al., 2013; Margolis and Spradling, 1995; Nystul and Spradling, 2007; Reilein et al., 2017; Song and Xie, 2002), demarcated as the boundary between the two adjacent cysts in Region 2a and the first single-file cyst in Region 2b. A recent study suggested that additional FSCs or their progeny may also reside in Region 2a (Reilein et al., 2017), but we are focusing here on those at the Region 2a/2b border for consistency with previous studies on Wnt signaling in FSCs (Dai et al., 2017; Sahai-Hernandez and Nystul, 2013; Wang and Page-McCaw, 2014). FSC divisions give rise to prefollicle cells (pFCs) that go on to differentiate into main body follicle cells, which encapsulate each germline cyst to produce the follicle; polar cells, which provide signals to pattern the follicle; or stalk cells, which form the connections between consecutive follicles.

The Wnt and EGFR pathways function as necessary and specific FSC niche signals. Both pathways are active in FSCs and required for self-renewal, but must be downregulated in pFCs that have moved downstream from the niche to allow for differentiation (Castanieto et al., 2014; Sahai-Hernandez and Nystul, 2013; Song and Xie, 2003; Wang and Page-McCaw, 2014). A recent study demonstrated that Wnt signaling is also active in early pFCs at the Region 2a/2b border, where it may function to preserve the capacity of these cells to differentiate toward the polar and stalk cell fates (Dai et al., 2017). Taken together, these findings demonstrate that there is a steep gradient of Wnt and EGFR signaling at the Region 2a/2b border, and that this pattern is important to specify the FSC and pFC fates. However, it is unclear how this pattern of signaling is maintained.

Here, we demonstrate that the specificity of Wnt signaling in the FSC niche at the Region 2a/2b border is due to spatial restriction of the Wnt ligand, Wingless (Wg), to the FSC niche. In addition, we find that Wnt signaling is required for EGFR pathway activity and that constitutive activation of EGFR partially rescues the self-renewal defect caused by loss of Wnt signaling. Lastly, we show that Wnt signaling is required for expression of the EGFR ligand, Spitz (Spi), in the early FSC lineage, and that Spitz promotes EGFR signaling in FSCs. Collectively, these results support a model in which Wg and

Center for Reproductive Sciences, Departments of Anatomy and OB/GYN-RS, University of California, San Francisco, CA 94143-0452, USA.

*Author for correspondence (todd.nystul@ucsf.edu)

R.P.K.-Y., 0000-0002-6250-2394; T.G.N., 0000-0002-6250-2394

Received 7 June 2018; Accepted 29 October 2018

Development (2018) 145, dev168716. doi:10.1242/dev.168716

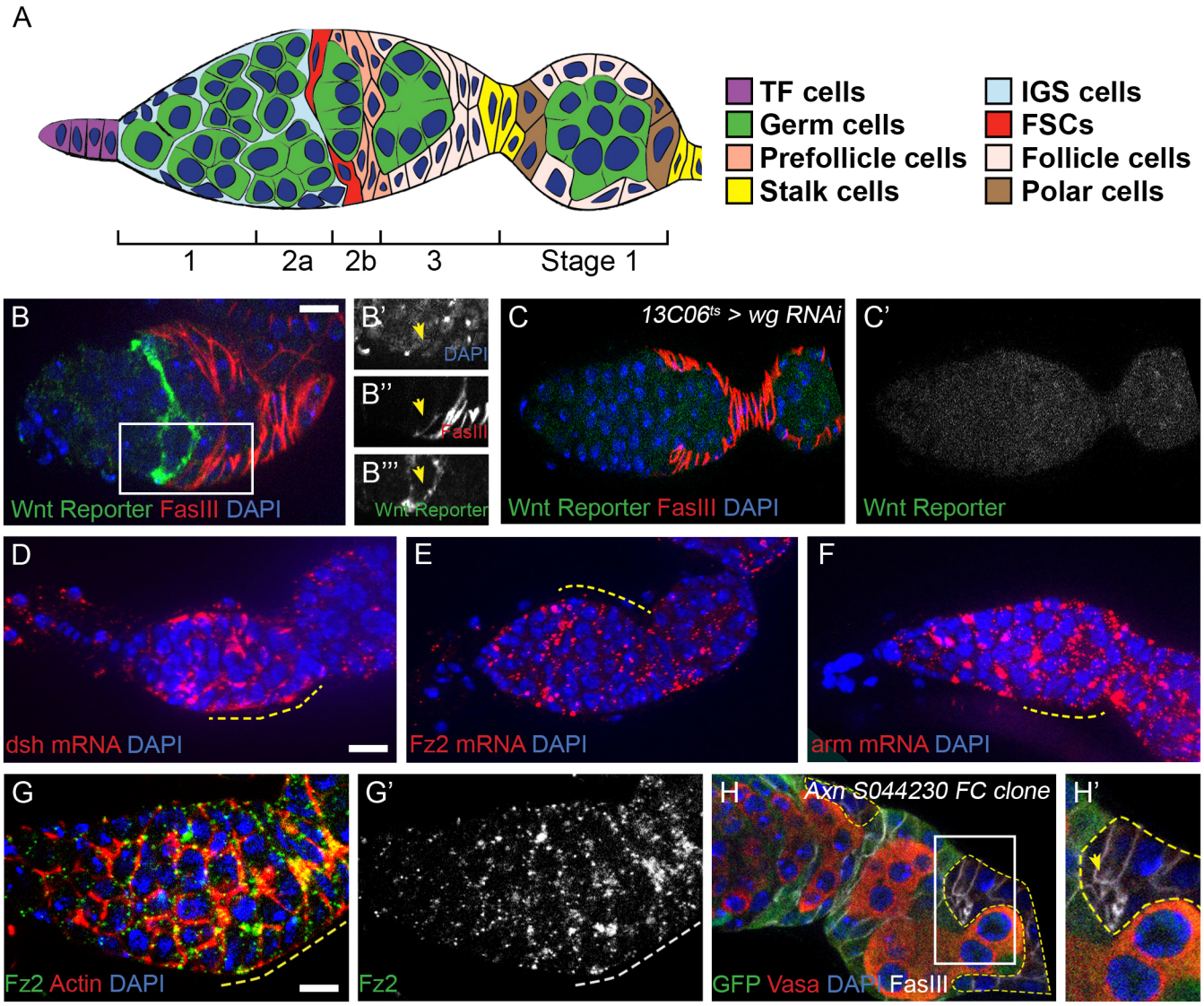

Fig. 1. Prefollicle cells are competent to transduce Wnt signaling but do not do so in wild-type tissue. (A) Diagram of the germarium. Follicle stem cells (red) are located at the Region 2a/2b border. FSCs produce pFCs (dark pink) that differentiate into main body cells (light pink), stalk cells (yellow) and polar cells (brown). Directly anterior to FSCs are IGS cells (light blue) which promote the development of the germ cell cysts (green) until they reach the Region 2a/2b border to acquire a follicle cell covering. (B) A germarium from the 3×GRH-4TH-GFP Wnt signaling reporter line stained for FasIII (red), GFP (reporter, green) and DAPI (blue). The DAPI, FasIII and Wnt reporter channels are shown separately in B′-B‴, respectively. The FSC (yellow arrow, B′-B‴) is identified as the anteriormost cell with FasIII staining (B″). GFP is detectable in the FSC but not in the immediately adjacent pFCs (right of the arrow). 64% of germaria showed this pattern of reporter expression (*N*=79). (C) RNAi knockdown of *wg* using the IGS cell driver 13C06-Gal4 eliminates 3×GRH-4TH-GFP reporter activation in the IGS cells and follicle stem cells of 83% of germaria (*N*=70). (D-F) Wild-type germaria stained with a FISH probe (red) for *dsh* mRNA (D), *fz2* mRNA (E) and *arm* mRNA (F), and DAPI (blue) reveals expression of Wnt pathway genes in FSCs and pFCs (dashed lines). Images are maximum-intensity *z*-projections of five 1 µm slices. (G,G′) Wild-type germarium stained for Fz2 protein (green), actin (red) and DAPI (blue). The Fz2 signal is present throughout the germarium, including in Regions 2b and 3 (dashed lines), where the FSCs and pFCs are located. (H) Germaria with $Axn^{S044230}$ mutant follicle cell clones stained for FasIII (white), GFP (clonal marker, green), Vasa (red) and DAPI (blue). The boxed area is shown enlarged in H′. GFP^{-} follicle cell clones exhibit multilayering consistent with Wnt pathway overactivation. Scale bars: 5 µm.

EGFR are activated specifically in stem cells by short-range signaling, and function in a signaling hierarchy to promote FSC self-renewal.

RESULTS

Multiple reporters demonstrate that Wnt signaling in the FSC niche region depends on Wg from ISCs

In canonical Wnt signaling, binding of a Wnt ligand to a Frizzled receptor results in recruitment of the positive regulator, *disheveled* (*dsh*), and the inhibition of the destruction complex, which limits pathway activity by targeting β-catenin for ubiquitin-mediated degradation. Thus, inhibition of the destruction complex allows β-catenin to accumulate in the nucleus, where it interacts with TCF (Pan – FlyBase) and regulates target gene expression in a cell type-specific manner (Clevers et al., 2014; van Amerongen and Nusse, 2009). Several reporter lines have been constructed that allow for monitoring of Wnt signaling *in vivo*. Two lines, *notum-lacZ* and *frizzled3-RFP* (*fz3-RFP*), that report the expression of a canonical Wnt pathway target gene as an indicator of pathway activity have been shown to have similar expression patterns in the germarium, although *fz3-RFP* is expressed more broadly and consistently

Development (2018) 145, dev168716. doi:10.1242/dev.168716

(Dai et al., 2017; Sahai-Hernandez and Nystul, 2013; Wang and Page-McCaw, 2014). Both reporters are expressed strongly in FSCs and then rapidly downregulated in pFCs that have moved downstream from the FSC niche. However, whereas *fz3-RFP* is expressed consistently throughout all IGS cells but not in cap or terminal filament cells (Fig. S1A,B), *notum-lacZ* is expressed only sporadically in terminal filament cells, cap cells, outer muscle sheath cells and IGS cells (Dai et al., 2017; Sahai-Hernandez and Nystul, 2013; Wang and Page-McCaw, 2014). To confirm the pattern of Wnt signaling in the FSC lineage, we investigated the expression pattern of a recently developed synthetic reporter, *3×GRH-4TH-GFP* (Zhang et al., 2014). This reporter contains four TCF binding sites (4TH) that facilitate TCF-driven GFP expression upon pathway activation in combination with three grainyhead binding sites (3×GRH) that repress GFP expression in the absence of Wnt pathway activity. This combination makes the reporter both highly sensitive to, and specific for, activation by TCF. We found that *3×GRH-4TH-GFP* is detectable in posterior IGS cells and FSCs at the Region 2a/2b border, identified as either the anteriormost FasIII^{+} cells (Fig. 1B) or the anteriormost cell in a negatively marked FSC clone (Fig. S1C), but not in cap or terminal filament cells, germ cells or pFCs in Region 2b or beyond. Thus, all three reporters indicate that there is a sharp drop in Wnt signaling at the Region 2a/2b border, with clearly detectable levels in the FSCs at the anterior edge of the FasIII border, and little or no signal in the pFCs immediately downstream.

We demonstrated previously that IGS cells are the predominant source of Wg for Wnt signaling in FSCs (Sahai-Hernandez and Nystul, 2013). To confirm this observation with the other two reporters, we combined *3×GRH-4TH-GFP* or *fz3-RFP* with *UAS-wg RNAi*, *tub-Gal80^{ts}*, and either *13C06-Gal4*, which is expressed in IGS cells, FSCs and pFCs near the Region 2a/2b border, or the follicle cell driver *109-30-Gal4* (Hartman et al., 2010). We grew the flies at 18°C to inhibit Gal4 activity during development, and then shifted adult flies to 29°C for 7 days to inhibit Gal80 and drive expression of *wg* small interfering RNA (siRNA). We found that expression of *wg* siRNA with *109-30-Gal4* caused only a mild reduction in the level of *3×GRH-4TH-GFP*, and had no effect on *fz3-RFP* expression (Fig. S2A-B′). In contrast, expression of *wg* siRNA with *13C06-Gal4* eliminated expression of *3×GRH-4TH-GFP* and *fz3-RFP* in the FSC niche region (Fig. 1C, Fig. S2C-D′). Interestingly, expression of *wg* siRNA with *13C06-Gal4* substantially reduced *fz3-RFP* expression but did not eliminate the signal entirely, consistent with reports that there are other Wnt ligands that promote Wnt signaling in IGS cells (Upadhyay et al., 2016, 2018; Wang and Page-McCaw, 2018; Wang et al., 2015). These observations indicate that the *3×GRH-4TH-GFP* reporter is responsive to Wnt signaling in the germarium, as expected, and provide confirmation of our previous finding that Wg produced by IGS cells is required for Wnt signaling in FSCs.

FSCs and follicle cells are competent to transduce Wnt signaling

We considered several possibilities for how a steep gradient of Wnt signaling could be maintained at the Region 2a/2b border. First, we investigated whether pFCs express Wnt pathway components and are capable of transducing a Wnt signal. β-catenin is ubiquitously expressed in epithelial cells, and several studies have reported the expression of Armadillo (Arm, the *Drosophila* homolog of β-catenin) protein in follicle cells (Kronen et al., 2014; Song and Xie, 2002). We detected transcripts of *dsh*, *frizzled2* (*fz2*) and *arm* by fluorescence *in situ* hybridization (FISH), as well as Fz2 protein in the FSCs and all follicle cells in the germarium (Fig. 1D-G′, Fig. S1D). Thus, both FSCs and pFCs express key positive regulators of Wnt signaling. In addition, we confirmed that pFC clones that were homozygous mutant for an essential component of the destruction complex, *Axin* (*Axn*), exhibited a multilayering phenotype (Fig. 1H) (Dai et al., 2017; Song and Xie, 2003). As discussed further below, we found that overexpression of *wg* causes a similar multilayering phenotype and the activation of the Wnt pathway reporter, 3×GRH-4TH-GFP, in pFCs (Fig. 3H-I′). Taken together, these findings indicate that the specificity of Wnt signaling for the FSC niche is not due to an inability of pFCs to transduce a Wnt signal.

Wnt signaling in FSCs is activated primarily by Wg and not regulated by the EGFR or Notch pathways

Second, we investigated whether the pattern of Wnt signaling in the FSC lineage is caused by interactions with other pathways or by the expression of other Wnt ligands, which could have either activating or inhibitory effects. Both EGFR and Notch signaling are known to interact with Wnt signaling in other tissues (Cordero et al., 2012; Freeman and Bienz, 2001; Hing et al., 1994; Hu and Li, 2010; Nagaraj and Banerjee, 2009; Szüts et al., 1997) and have spatially restricted activity in the FSC lineage (Castanieto et al., 2014; Sahai-Hernandez and Nystul, 2013). In addition, EGFR signaling is required for self-renewal (Castanieto et al., 2014), and Notch signaling cooperates with Wnt signaling to pattern pFC differentiation (Dai et al., 2017). Thus, we tested whether perturbations of either pathway altered the pattern of Wnt signaling. We found that expression of EGFR siRNA with *109-30-Gal4* substantially reduced EGFR protein levels (Fig. S6B), but did not change the pattern of *3×GRH-4TH-GFP* expression (Fig. 2A-B′). Likewise, RNAi knockdown of *Notch* or constitutive activation of EGFR in follicle cells caused the morphological defects expected from previous reports (Castanieto et al., 2014; Johnston et al., 2016; Lopez-Schier and St Johnston, 2001), but did not affect the pattern of *3×GRH-4TH-GFP* expression (Fig. 2C-D′).

There are seven known Wnt ligands in the *Drosophila* genome (Swarup and Verheyen, 2012), including Wg, and three (Wnt2, Wnt4 and Wnt6) have been recently found to be important for Wnt signaling in anterior IGS cells (Hamada-Kawaguchi et al., 2014; Upadhyay et al., 2016; Wang et al., 2015). Of these, Wnt2 and Wnt4 are required in IGS cells (Upadhyay et al., 2016, 2018; Wang et al., 2015), and Wnt6 is required in cap and terminal filament cells (Wang and Page-McCaw, 2018). To test whether any other Wnt ligand besides Wg affects Wnt signaling in the FSC, we performed RNAi knockdown of each ligand using *13C06-Gal4*. RNAi knockdown of *Wnt3/5*, *Wnt6*, *Wnt8* or *Wnt10* did not cause an observable follicle cell phenotype (Fig. S3A-D), although we could not confirm that the knockdown was effective in these cases. Knockdown of *Wnt2* or *Wnt4* caused germ cell differentiation defects, as reported previously, but did not cause an observable follicle cell phenotype (Fig. S3E-I). Interestingly, we found that *Wnt4* knockdown, but not *Wnt2* knockdown, also diminished expression of *3×GRH-4TH-GFP* (Fig. S3J-L′), indicating that *wg* and *Wnt4* have nonredundant roles in activating Wnt signaling to a level that is detectable with this reporter. However, because *Wnt4* knockdown did not cause a follicle cell phenotype, it is likely that Wnt signaling in FSCs was not abrogated entirely. These data indicate that the pattern of Wnt signaling in the early FSC lineage is not dependent upon EGFR or Notch pathway activity, and suggest that Wnt pathway is activated in FSCs primarily by Wg, with more minor contributions from Wnt4.

Wnt signaling is spatially restricted in the germarium

Third, we investigated whether the pattern of Wnt signaling in the FSC lineage is due to the restriction of Wg movement through the

Development (2018) 145, dev168716. doi:10.1242/dev.168716

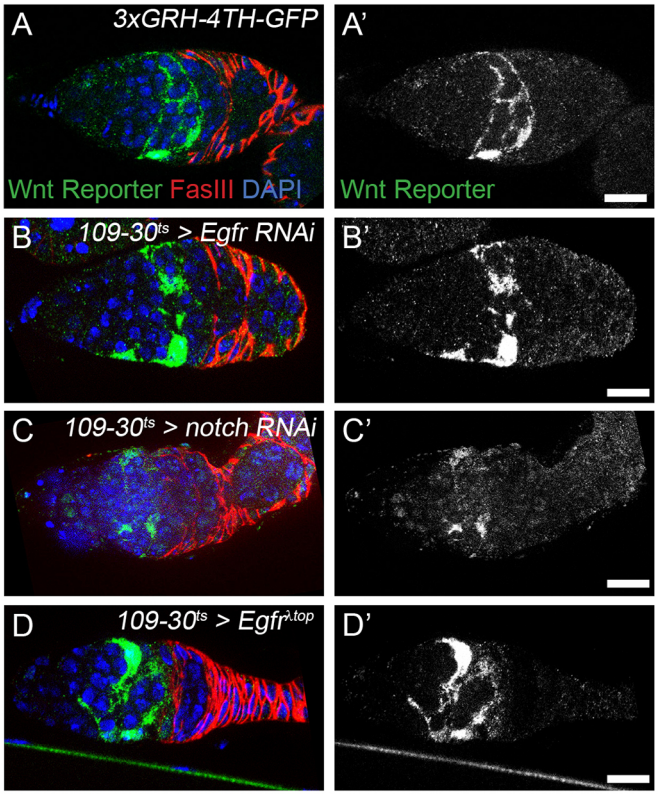

Fig. 2. Perturbations of EGFR or Notch signaling pathways do not affect the Wnt signaling reporter. (A-D) Germaria with the *3×GRH-4TH-GFP* reporter line either alone as a control (A) or combined with *109-30-Gal4*, *tub-Gal80^{ts}* to restrict expression to adulthood, and *UAS-Egfr RNAi* (B), *UAS-Notch-RNAi* (C) or *Egfr$^{λ.top}$* stained for FasIII (red), GFP (green) and DAPI (blue). The Wnt reporter channel is shown separately in A′, B′, C′ and D′. RNAi knockdown of EGFR or Notch, or expression of constitutively active EGFR (*Egfr$^{λ.top}$*) does not affect the pattern of 3×GRH-4TH-GFP expression. Scale bars: 5 µm.

tissue. *wg* transcript is detectable in terminal filament cells, cap cells and IGS cells, but protein levels, as assayed by immunofluorescence, are highest at the anterior tip of the germarium and taper off toward the posterior, becoming undetectable by Region 2b (Fig. S4A) (Sahai-Hernandez and Nystul, 2013; Wang and Page-McCaw, 2014). To determine whether Wg produced in the anterior half of the germarium can move beyond the Region 2a/2b border, we simultaneously overexpressed hemagglutinin (HA)-tagged Wg (*HA::wg*) and *CD8::GFP* with *13C06-Gal4* using *tub-Gal80^{ts}* to restrict expression to adulthood. We co-stained ovaries from control and experimental groups for HA and GFP, and found that, whereas the HA signal was diffuse and nonspecific in control ovaries without a Gal4 driver (Fig. 3A), bright HA::Wg signal was clearly detectable in the experimental ovaries and almost entirely confined to the *13C06-Gal4*-expressing cells, as identified by *CD8::GFP* expression, with little or no signal visible beyond the boundary of this domain (Fig. 3D, Fig. S4B). In addition, similar to control ovaries (Fig. 3B-C′), overexpression of *HA::wg* with *13C06-Gal4* did not cause pFC overproliferation or differentiation defects (Fig. 3E, Fig. S4C), and *3×GRH-4TH-GFP* was not activated in pFCs (Fig. 3F, Fig. S4B). In contrast, overexpression of *HA::wg* during adulthood with *109-30-Gal4* produced detectable levels of HA::Wg specifically within the *109-30-Gal4* expression region (Fig. 3G), and resulted in severe morphological phenotypes in the follicle epithelium that phenocopied the loss of components of the destruction complex (Fig. 1H) (Song and Xie, 2003). Specifically, overexpression of *HA::wg* in follicle cells caused the germaria to become substantially larger as follicles fused together and failed to bud properly, and follicle cells to accumulate in disorganized clusters (Fig. 3H, Fig. S4C). In addition, the *3×GRH-4TH-GFP* reporter was ectopically activated in pFCs (Fig. 3I,I′). These observations provide further evidence that pFCs are capable of activating Wnt signaling and demonstrate that HA::Wg is functional. Taken together, these data indicate that Wg ligand is spatially restricted, such that, even in the overexpression case, Wg produced in IGS cells does not activate Wnt signaling beyond the Region 2a/2b border.

A recent study proposed that cap and terminal filament cells are an important source of Wg for the FSC niche (Wang and Page-McCaw, 2014). This conclusion was based on the observation that overexpression of *wg* using the cap and terminal filament cell driver, *bab1-Gal4*, resulted in an overproduction of stalk cells, whereas expression of *wg* siRNA with *heat shock-Gal4* (*hs-Gal4*) caused a fused follicle phenotype that is suggestive of an underproduction of follicle cells. However, *bab1-Gal4* is also expressed during ovarian development, and *hs-Gal4* is expressed in all cells upon heat shock, so these experiments lacked either spatial or temporal precision. In addition, this conclusion is inconsistent with our previous finding that RNAi knockdown of *wg* from cap and terminal filament cells specifically during adulthood using *bab1-Gal4* and *tub-Gal80^{ts}* is not sufficient to cause a follicle cell phenotype or eliminate *notum-lacZ* expression (Sahai-Hernandez and Nystul, 2013). Therefore, to investigate further, we repeated the knockdown or overexpression of *wg* using *bab1-Gal4* and *tub-Gal80^{ts}* and looked for the phenotypes described in this study. We found that overexpression of *HA::wg* with *bab1-Gal4* specifically during adulthood produced clearly detectable levels of HA::Wg at the anterior tip of the germarium, indicating that the protein was expressed in the expected region, but did not cause an overproduction of stalk cells or any other detectable follicle cell phenotype (Fig. 4A-B′). In addition, RNAi knockdown of *wg* specifically during adulthood using *bab1-Gal4* did not cause follicle formation defects, and did not affect *fz3-RFP* expression in IGS cells or FSCs (Fig. 4C).

As an additional test of the range of Wg in the germarium, we examined the ovaries of *Nrt::wg* flies, in which the endogenous *wg* gene has been replaced with a gene encoding for a fusion of the transmembrane protein Neurotactin (Nrt) and Wg (Alexandre et al., 2014). This targets the fusion protein to the plasma membrane so that its ability to activate Wnt signaling in nonadjacent cells is substantially reduced or eliminated. *Nrt::wg* homozygous flies are viable and grow to adulthood with normally patterned wings, although they are smaller and substantially less fit than their wild-type siblings (Alexandre et al., 2014). In addition, we found that the ovaries of *Nrt::wg* homozygotes were much smaller than those of their heterozygous siblings, and that homozygotes laid fewer eggs, many of which did not hatch into larvae. However, the germaria were morphologically normal, with pERK^{+} (RI^{+}) FSCs (Fig. 4D) and a normal pattern of expression of the differentiation factors *castor* (*cas*) and *eyes absent* (*eya*) (Fig. 4E) (Chang et al., 2013). In addition, we observed 5-ethynyl-2′-deoxyuridine (EdU) incorporation into FSCs and pFCs, indicating that these cells are proliferative (Fig. 4F). These findings confirm that the cap and terminal filament cells are not a major source of Wg for the FSC niche. Taken together, our data strongly suggest that the specificity of Wnt signaling in FSCs is due to a short-range Wg signal from *13C06-Gal4*-expressing cells, combined with spatial restriction of Wg movement across this region.

Development (2018) 145, dev168716. doi:10.1242/dev.168716

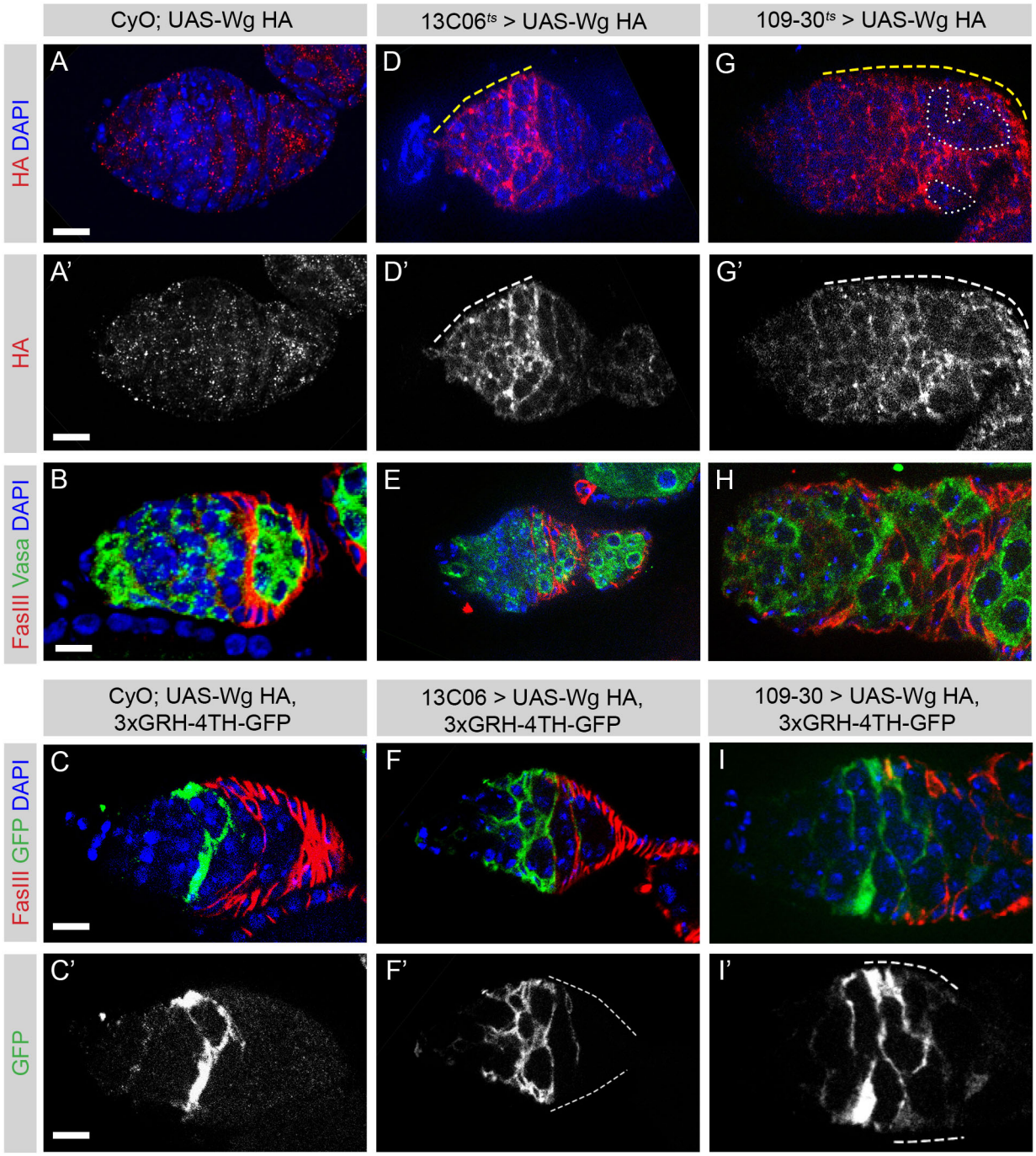

Fig. 3. Wingless ligand is spatially restricted to the Region 2a/2b border. (A-I) Germaria with *UAS-wg::HA* without a Gal4 driver, as a control (A-C), or with *13C06-Gal4* (D-F′) or *109-30-Gal4* (G-I). In addition, germaria in C, F and I have the *3×GRH-4TH-GFP* reporter. Germaria in panels A, D and G are stained for HA (red) and DAPI (blue). The HA channel is shown separately in A′, D′ and G′. White dotted lines outline germ cell cysts in G and G′. Germaria in B, E and H are stained for FasIII (red), Vasa (green) and DAPI (blue). Germaria in panels C, F and I are stained for FasIII (red), GFP (green) and DAPI (blue). The GFP channel is shown separately in C′, F′ and I′. Overexpression of *HA::wg* with *13C06-Gal4* does not cause a follicle cell phenotype, and GFP expression is expanded in Region 2a but remains almost entirely inactive in Regions 2b and 3 (dashed lines). In contrast, overexpression with *109-30-Gal4* causes follicle formation defects, resulting in an enlarged ovariole and substantial upregulation of GFP expression in Regions 2b and 3 (dashed lines). Scale bars: 5 µm.

Wnt signaling promotes EGFR signaling in FSCs

We found previously that EGFR signaling is necessary for FSC maintenance, and that pERK, a marker of EGFR signaling, is detectable in IGS cells, FSCs and pFCs along the Region 2a/2b border, but rarely in pFCs in Region 2b (Castanieto et al., 2014). In addition, we have since noticed that pERK is also detectable sporadically in Region 3 follicle cells. To determine whether Wnt signaling is required for EGFR signaling, we generated FSC clones that are homozygous mutant for arm^{8}, arm^{F} or dsh^{3}. arm^{8} is a hypomorph that impairs Wnt signaling but not cell-cell adhesion (Llimargas, 2000), and arm^{F} and dsh^{3} are null alleles (Haelterman et al., 2014; Perrimon and Mahowald, 1987; Yamamoto et al.,

Development (2018) 145, dev168716. doi:10.1242/dev.168716

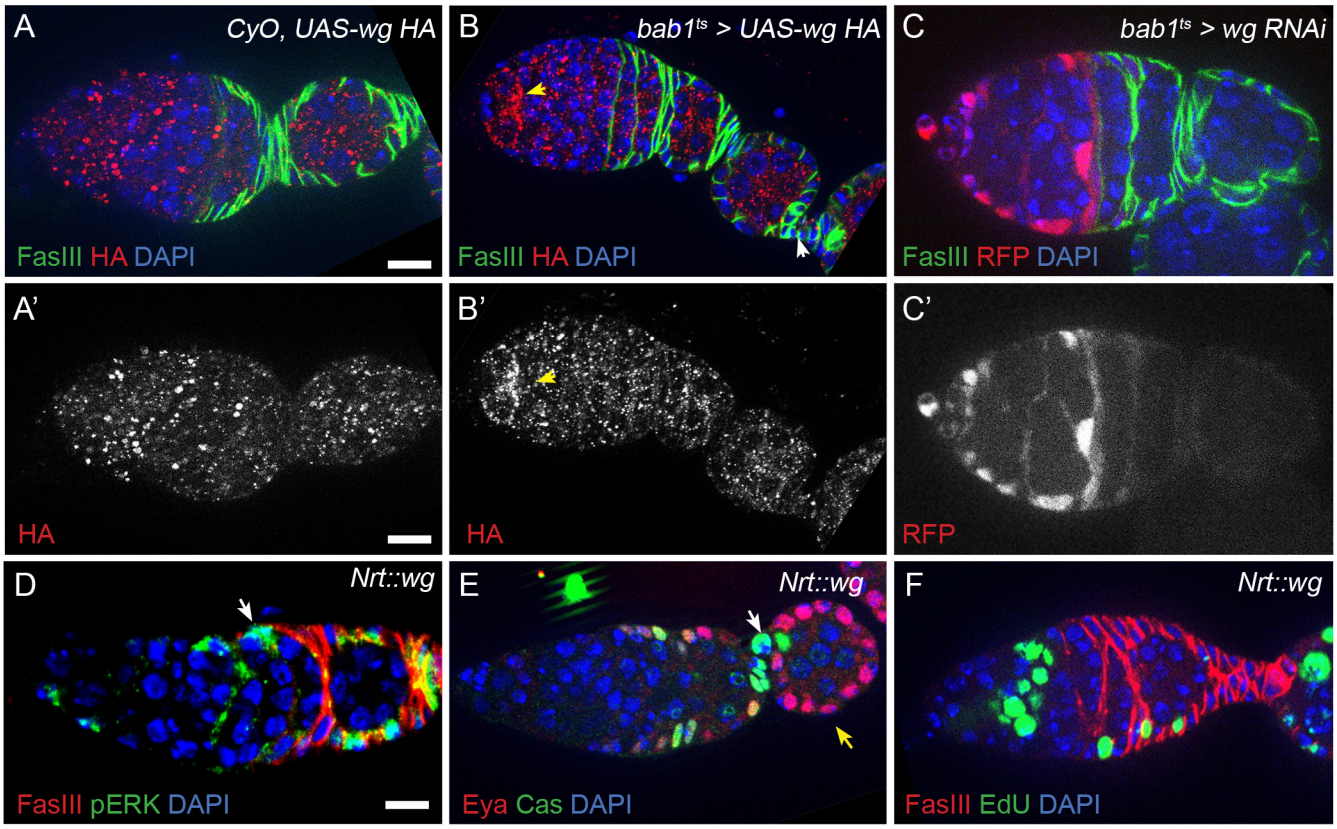

Fig. 4. Juxtacrine signaling is sufficient for the FSC niche. (A,B) *UAS-HA::wg* germaria without a Gal4 driver as a control (A) or with *bab1-Gal4* and *tub-Gal80^{ts}* to restrict expression to adulthood (B), which is expressed in cap and terminal filament cells, stained for HA (red), FasIII (green) and DAPI (blue). The HA channel is shown separately in A′ and B′. Overexpression with *bab1-Gal4* results in accumulation of HA::Wg in the anterior of the germarium (yellow arrows) but does not cause a follicle cell phenotype, including in the stalk cells (white arrow). (C) Germaria with the *fz3-RFP* reporter, *bab1-Gal4* driving expression of *wg* siRNA, and *tub-Gal80^{ts}* to restrict expression to adulthood stained for RFP (red), FasIII (green) and DAPI (blue). Expression of *wg* siRNA with *bab1-Gal4* does not affect *fz3-RFP* reporter expression in IGS and FSCs. The RFP channel is shown separately in C′. (D,E) Germaria from *Nrt::wg* homozygous flies stained with DAPI (blue) and either FasIII (red) and pERK (green) (D), or Eya (red) and Cas (green) (E). (F) An EdU assay to identify proliferating cells in an *Nrt::wg* homozygous germarium stained for FasIII (red), EdU (green) and DAPI (blue). Niche function and pFC differentiation appears unaffected in *Nrt::wg* homozygotes as these germaria have a normal pattern of pERK in FSCs (D, white arrow) and IGS cells; normal pFC morphology as visualized with FasIII staining (D,F); normal segregation of the *cas* and *eya* expression from a Cas^{+}, Eya^{+} state in pFCs to Cas^{-}, Eya^{+} stalk cells (E, white arrow), and Cas^{-}, Eya^{+} follicle cells (E, yellow arrow); and contain proliferative (EdU^{+}) pFCs (F, green). Scale bars: 5 µm.

2014). We found that the pERK signal was diffuse and indistinguishable from background in most *arm* or *dsh* mutant (GFP^{-}) FSCs, whereas a nuclear pERK signal was clearly detectable in nearly all of the heterozygous (GFP^{+}) FSCs in the same germaria (Fig. 5A-B‴,D, Fig. S5). FSCs that are homozygous mutant for *arm* or *dsh* are lost from the niche at an increased rate (Song and Xie, 2003), so it is possible that the loss of pERK in these cells is due to a general decrease in receptivity to niche signals prior to their exit from the FSC niche at the Region 2a/2b border. However, homozygosity for *Axn^{S044230}*, which causes constitutive activation of Wnt signaling, also causes an increased rate of FSC loss (Song and Xie, 2003), and yet we found that these mutant FSCs typically remained pERK^{+} (Fig. 5C-D). This suggests that the loss of pERK in *arm* or *dsh* mutant FSCs is not a general feature of mutations that increase the rate of FSC loss from the niche, but is instead specifically caused by decreased Wnt signaling. As an additional test, we assayed for pERK in germaria upon RNAi knockdown of *arm* in the FSCs and all follicle cells in the germarium using *109-30-Gal4*, and found that pERK was undetectable in FSCs in the majority of germaria (Fig. 5E-F). Collectively, these data strongly suggest that Wnt signaling is required for EGFR signaling in FSCs.

Constitutively active EGFR signaling partially suppresses FSC loss in the absence of Wnt signaling

Because both EGFR and Wnt signaling are required for FSC self-renewal (Castanieto et al., 2014; Song and Xie, 2003), we considered whether reduced EGFR signaling contributes to the loss of self-renewal in Wnt pathway mutants. To test this possibility, we performed standard FSC self-renewal assays (Kronen et al., 2014; Song and Xie, 2003), in which sparse wild-type or mutant FSC clones are induced during adulthood, and the change in clone frequency is quantified over time. We used the mosaic analysis with a repressible cell marker (MARCM) system (Lee and Luo, 2001) to produce clones that are positively marked by the expression of CD8::GFP, and quantified the change in clone frequency at 7, 14 and 21 days after clone induction (Fig. 6A). Consistent with previous reports (Song and Xie, 2003), the proportion of germaria with *dsh^{3}* FSC clones decreased at significantly higher rates compared with the wild-type control (Fig. 6B). Interestingly, overexpression of the constitutively active *Egfr$^{\lambda top}$* allele in *dsh^{3}* clones restored the pERK signal (Fig. 6C) and significantly decreased the rate of FSC clone loss (Fig. 6B), although the frequencies of *Egfr$^{\lambda top}$*, *dsh^{3}* double mutant clones were still lower than those of the wild-type control. These findings indicate that the signaling steps between EGFR activation

Development (2018) 145, dev168716. doi:10.1242/dev.168716

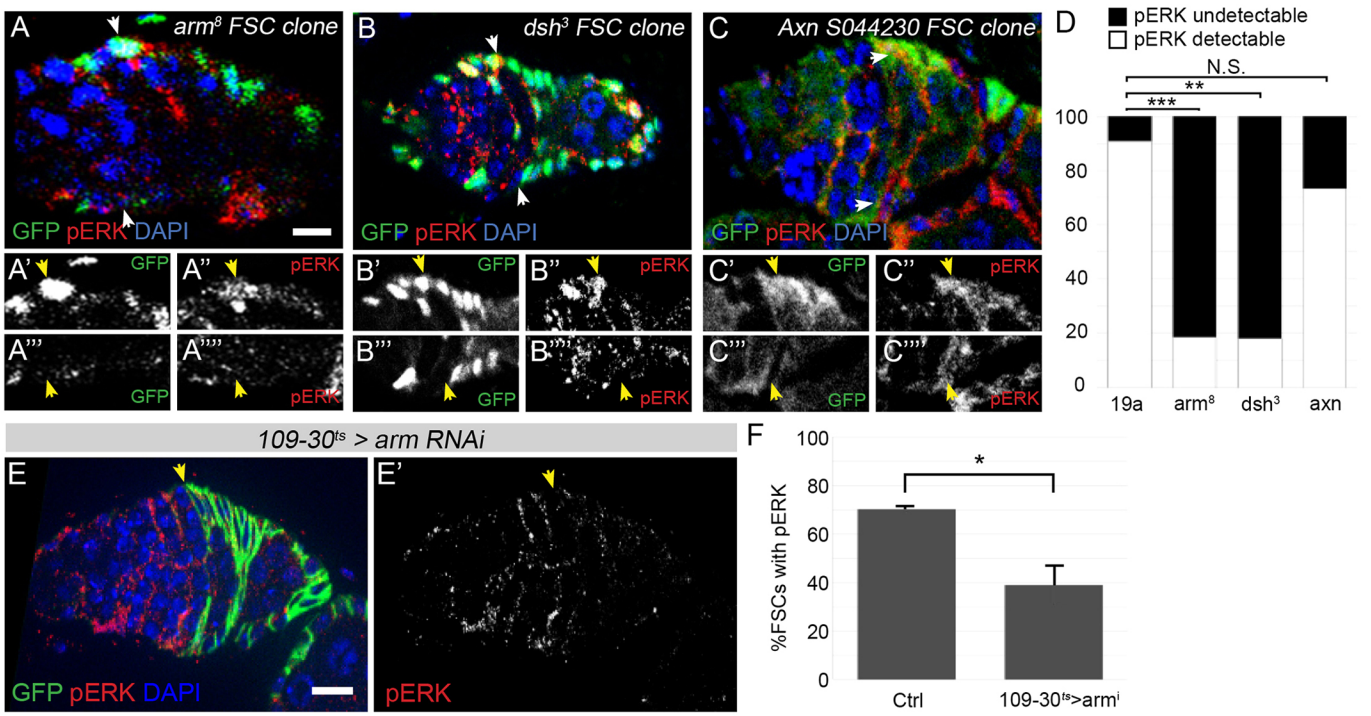

Fig. 5. Wnt signaling components are required for pERK in FSCs. (A-C) Germaria with *arm*^{8} (A), *dsh*^{3} (B) or *axn*^{S044230} (C) clones stained for pERK (red), GFP (clonal marker, green) and DAPI (blue). Images are oriented with a GFP^{+} (wild-type) FSC on top and a GFP^{-} (homozygous mutant) FSC on the bottom. FSCs (white arrows) are identified as the anteriormost cell in an FSC clone and by their position at the Region 2a/2b border. Wild-type control FSCs are pERK^{+} in each case, whereas *arm*^{8} and *dsh*^{3} FSCs are pERK^{-}. In contrast, *axn*^{S044230} FSCs are pERK^{+}. The GFP channel is shown separately in A′, A‴, B′, B‴, C′ and C‴; the pERK channel is shown separately in A″, A⁗, B″, B⁗, C″ and C⁗. (D) Quantification of germaria with pERK^{+} GFP^{-} FSCs in germaria in which the wild-type (GFP^{+}) FSC is pERK^{+} for the indicated genotypes. ***P*<0.01, ****P*<0.001 and N.S. indicates not significant, using a two-sided Fisher's Exact test. (E) Expression of *arm* siRNA with the follicle cell driver 109-30-Gal4 causes a similar reduction in pERK staining in FSCs (yellow arrow). The pERK channel is shown separately in E′. (F) Quantification of *arm* RNAi FSCs with undetectable nuclear pERK compared with siblings that lack the driver. Error bars represent 1 s.d. **P*<0.05, using a paired Student's *t*-test where the null hypothesis is that the percentage of FSCs with pERK is not significantly different between control (+/cyo; UAS-arm RNAi/+) and *arm* RNAi. *N*=3 experiments, *n*>20 for each experiment. Scale bars: 5 µm.

and ERK phosphorylation do not require Wnt signaling, and that restoration of EGFR signaling can partially compensate for the self-renewal defect in *dsh*^{3} mutant FSCs.

Wnt promotes EGFR signaling via *spitz* transcription

To investigate how Wnt signaling functions genetically upstream of EGFR signaling, we first tested whether Wnt signaling is required for expression of EGFR. We found that EGFR is expressed throughout the FSC lineage in wild-type germaria (Fig. S6A-B′) and that this expression pattern was not affected by RNAi knockdown of *arm* or *dsh* (Fig. S6C-D′). Thus, Wnt signaling is not required for the expression of EGFR in FSCs or pFCs.

Next, we investigated whether Wnt signaling is required for the expression of the EGFR ligand, *spitz*. *spitz* is known to be expressed in the follicle cell lineage (Wasserman and Freeman, 1998), and we confirmed that *spitz* is expressed in follicle cells by FISH and with a *spitz-lacZ* enhancer trap (Fig. 7C, Fig. S7A-B′). In addition, we found that expression of *spitz* siRNA with *109-30-Gal4* eliminated pERK staining in a majority of FSCs and pFCs within Region 2b (Fig. 7A-B′,E), although it did not affect the pERK signal in follicle cells in Region 3 and later, where EGFR is likely activated by another EGFR ligand, such as *gurken* from the germline (Wasserman and Freeman, 1998). These results confirm that *spitz* is produced by cells in the FSC lineage and indicate that it is important for EGFR pathway activity in FSCs. In the intestine, Wnt operates via *dMyc* (*Myc*) to activate *spitz* (Cordero, et al., 2012). However, we found that RNAi knockdown of *dMyc* did not eliminate pERK in FSCs (Fig. S7C-D′), suggesting that this mechanism is not operating in the FSC lineage. Instead, we noticed that the chromatin immunoprecipitation with DNA sequencing (ChIPseq) data available on ModMINE (Contrino et al., 2012) indicate that there is a high confidence TCF binding site in the *spitz* gene that overlaps with the transcription start site of two *spitz* isoforms. We searched this sequence and identified three putative TCF-binding sites that are highly conserved across dipteran insect species (Fig. S7E,F), suggesting that *spitz* might be a direct target of TCF. Consistent with this, we found that expression of *arm* siRNA with *109-30-Gal4* substantially reduced *spitz-lacZ* expression in the FSCs and pFCs of most germaria (Fig. 7C-D′,F). Taken together, these results suggest a hierarchical structure of niche signals in which Wnt signaling promotes the activation of EGFR signaling in FSCs by inducing expression of *spitz* in FSCs and early pFCs.

DISCUSSION

In this study, we investigated the relationship between the Wnt and EGFR pathways in FSCs. Both pathways are known to be essential for FSC self-renewal and to inhibit pFC differentiation (Castanieto et al., 2014; Dai et al., 2017; Song and Xie, 2003), but how these pathways are regulated in the early FSC lineage is not well understood. Our data support a model in which the Wnt and EGFR pathways function in a signaling hierarchy, beginning with a short-range Wg signal from IGS cells that activates Wnt signaling in FSCs, which promotes expression of *spitz* in the early FSC lineage.

Development (2018) 145, dev168716. doi:10.1242/dev.168716

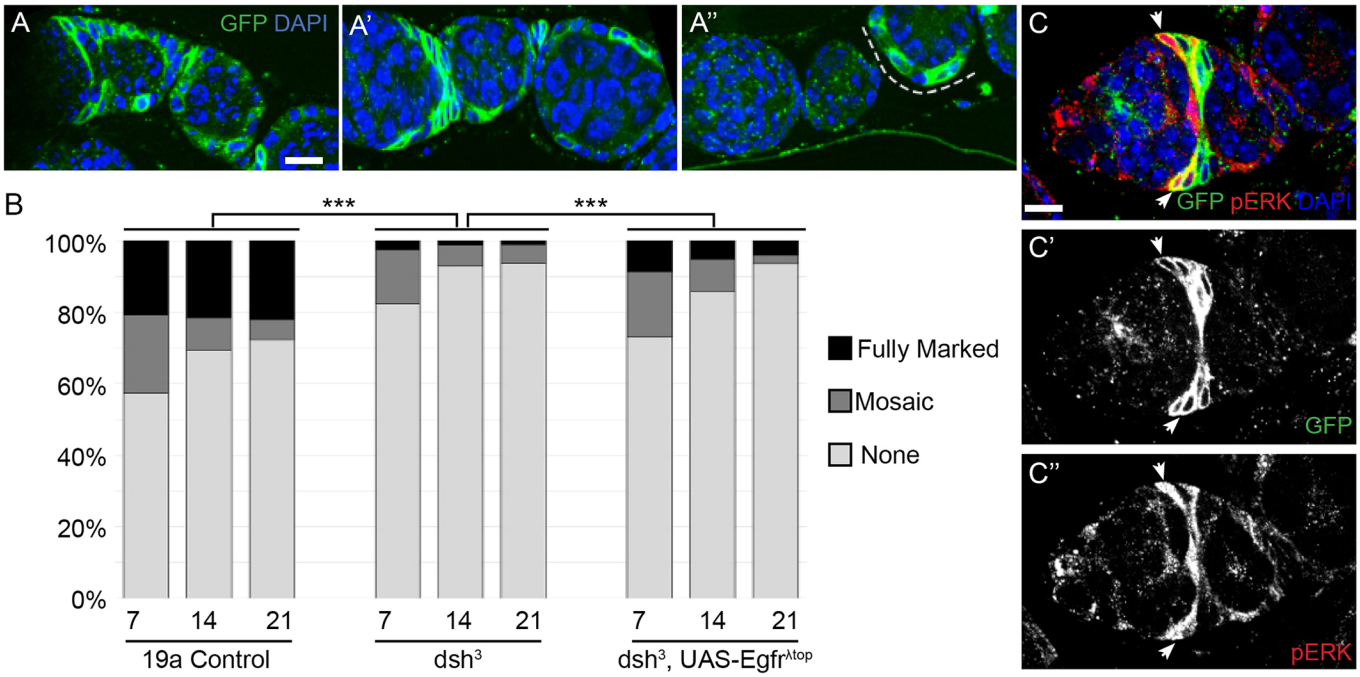

Fig. 6. Constitutive active EGFR signaling can partially rescue Wnt pathway mutations in FSCs. (A) Germaria with wild-type control MARCM clones stained for GFP (clone marker, green) and DAPI (blue) in which the germarium is fully marked (A), mosaic (A′) or fully unmarked (A″). A transient clone is visible in A″ (dashed line). (B) Lifespan assay for 19a control, *dsh*^{3} and *dsh*^{3} with *UAS-Egfr*$^{\lambda top}$. The proportions of germaria with fully marked, mosaic or fully unmarked FSCs labeled are indicated by light gray, dark gray and black bars, respectively. ***P<0.001 using Chi-squared tests for comparisons between indicated genotypes across all time points. Differences between genotypes at each time point are also significant (see Materials and Methods and Supplementary Data for P-values). n>250 germaria for each time point, for each genotype. (C) Germarium with a *dsh*^{3} *UAS-Egfr*$^{\lambda top}$ MARCM clone stained for pERK (red), GFP (clonal marker, green) and DAPI (blue). GFP and pERK channels are separated out in C′ and C″, respectively. pERK staining is restored in the double mutant FSCs (white arrows). FSCs are identified as the anteriormost cell in an FSC clone and by their position at the Region 2a/2b border. Scale bars: 5 µm.

This, in turn, leads to the activation of EGFR signaling in FSCs, which cooperates with Wnt signaling to promote FSC self-renewal. Several lines of evidence support this model. First, we have now shown with three separate Wnt reporters, two in this study and one previously (Sahai-Hernandez and Nystul, 2013), that Wg production by IGS cells is required for Wnt signaling in FSCs. As this is in contrast to a recent study that proposed a distant source of Wg for the FSC niche (Wang and Page-McCaw, 2014), we performed several additional tests of the range of Wg signaling in the germarium. We found that FSC niche function is not disrupted when Wg is tethered to the membrane, and that, even upon overexpression of *HA::wg*, both the pattern of Wnt pathway activity and the location of HA-tagged Wg are only detected within or very close to the expression domain of the Gal4 driver used. In contrast, overexpression of Wg in follicle cells causes significant pFC differentiation defects. This indicates that Wg movement in the germarium is substantially restricted and suggests that a short-range Wg signal is both necessary to allow for pFC differentiation and sufficient to promote FSC self-renewal. Although further study will be required to fully elucidate the mechanism by which the steep gradient of Wnt signaling at the Region 2a/2b border is maintained, our findings suggest that interactions with the EGFR and Notch pathways, or differences in the capacity of FSCs and downstream pFCs to transduce a Wnt signal, are not major factors in the patterning of Wnt activity within the early FSC lineage. Instead, recent studies suggest that proteins that interact with Wnt ligands in the extracellular space restrict the movement of Wnt ligands into the follicle epithelium. Specifically, RNAi knockdown of *Matrix metalloproteinase 2* during adulthood in cap, terminal filament and IGS cells causes follicle cell phenotypes (Wang and Page-McCaw, 2014), and RNAi knockdown of heparan sulfate proteoglycans using 109-30-Gal4 reduces *fz3-RFP* expression in FSCs (Su et al., 2018).

Second, we found that effectors of the Wnt pathway are required for EGFR signaling in FSCs. Our data suggest that this is due, in part, to a role for Wnt signaling in promoting the expression of *spitz* in the early FSC lineage. Indeed, we found that knockdown of *arm* substantially reduced *spitz-lacZ* expression in the follicle cells within the germarium, and knockdown of *spitz* eliminated the pERK signal in most FSCs. However, the failure of *spitz-RNAi* expression to eliminate pERK in all FSCs suggests that either the RNAi knockdown was incomplete or that there are other sources of EGFR ligand for the FSC niche. It is interesting that knockdown of *arm* decreased *spitz-lacZ* expression in follicle cells throughout the germarium, even though Wnt signaling is not normally active downstream of the Region 2a/2b border. This suggests that Wnt signaling is required in FSCs for both the activation of *spitz* expression in FSCs, as well as the continued *spitz* expression during the early stages of pFC differentiation. Consistent with this possibility, we and others have identified signaling genes that are required in FSCs, but not pFCs, for pFC differentiation (Castanieto et al., 2014; Li et al., 2010), suggesting that some signals that act on FSCs have effects that persist into the daughter cells. Alternatively, it could be that other functions of *arm*, such as its role in cell-cell adhesion, contribute to the regulation of *spitz* in pFCs. However, knockdown of *arm* did not affect *spitz-lacZ* expression in budded follicles, indicating that *spitz* expression becomes independent of *arm* function at that point.

Development (2018) 145, dev168716. doi:10.1242/dev.168716

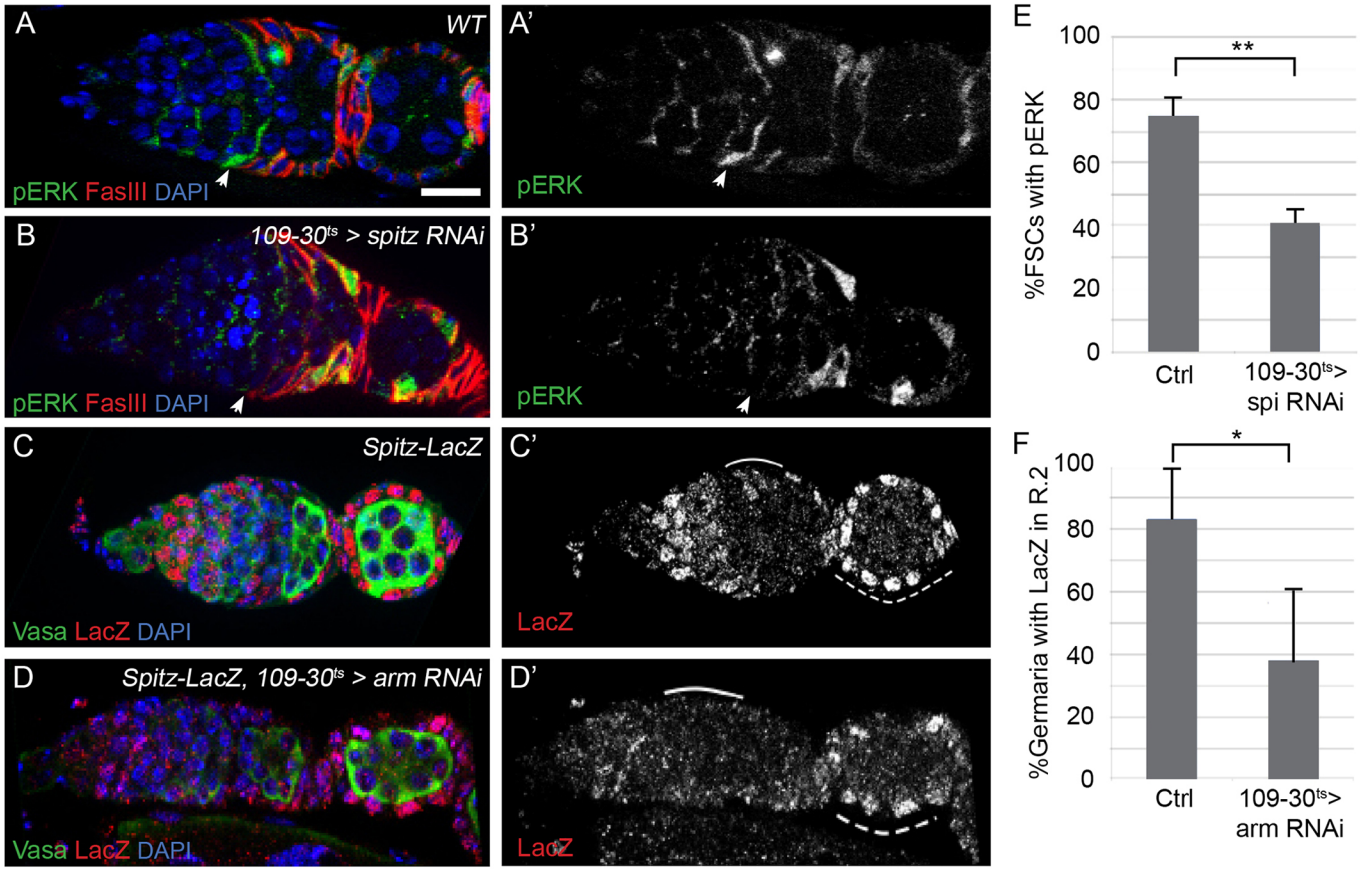

Fig. 7. Wnt signaling promotes transcription of the EGFR ligand *spitz*. (A,B) A wild-type germarium (A), or germarium with *spitz* siRNA driven by *109-30-Gal4* and with *tub-Gal80^{ts}* to restrict expression to adulthood (B) stained for pERK (green), FasIII (red) and DAPI (blue). Expression of *spitz* siRNA reduces pERK staining in FSCs (white arrows), identified as the anteriormost FasIII^{+} cells, but not in pFCs further downstream. The pERK channel is shown separately in A′ and B′. (C,D) A germarium with a *spitz-lacZ* enhancer trap either without (C) or with (D) expression of *arm* siRNA using *109-30-Gal4* and *tub-Gal80^{ts}* to restrict expression to adulthood stained for *lacZ* (red), Vasa (green) and DAPI (blue). (C′,D′) *spitz-lacZ* is normally expressed throughout the FSC lineage with lower expression in Region 2b and 3 (C′, white solid and dashed lines) and staining in Region 2b is substantially reduced upon knockdown of *arm* (D′, white solid line), with some staining still detectable in Region 3 (D′, white dashed line). (E,F) Quantification of the percentage of control or *spitz* RNAi germaria with pERK^{+} FSCs (E) and the percentage of control or *arm* RNAi germaria with at least one *lacZ*-positive nucleus in Region 2b (F). *P<0.05, **P<0.01, using a two-sided Student's *t*-test. Error bars represent 1 s.d. Scale bars: 5 µm.

Third, we tested the functional relationship between Wnt and EGFR signaling in FSC self-renewal and found that constitutive activation of EGFR signaling significantly decreases the rate at which *dsh^{3}* FSCs are lost from the niche. Although we cannot rule out that activation of EGFR signaling circumvents the loss of Wnt signaling in a manner that is unrelated to the relationship between these two pathways in wild-type FSCs, the most straightforward interpretation of this result is that Wnt signaling functions upstream of EGFR signaling to promote FSC self-renewal. However, Wnt signaling is likely to be important for other aspects of self-renewal as well. For example, a previous study found that overexpression of a constitutively active allele of the BMP receptor *thickveins* decreases the rate of *dsh^{3}* FSC loss (Kirilly et al., 2005), suggesting that Wnt signaling might also function upstream of BMP signaling to promote self-renewal.

Our findings here and previous studies (Wang and Page-McCaw, 2014) indicate that *fz3-RFP* expression is broader and more consistent than *notum-lacZ* or *3×GRH-4TH-GFP* expression in the germarium. Given the importance of Wnt signaling as an upstream activator of the FSC self-renewal program, it is likely that Wnt signaling is, in fact, active in all FSCs, as suggested by the *fz3-RFP* reporter. However, RFP has a relatively long half-life (Mirabella et al., 2004), so the variation in *notum-lacZ* and *3×GRH-4TH-GFP* expression could be revealing fluctuations in pathway activity that are not easily detectable with *fz3-RFP*. Interestingly, constitutive activation of Wnt signaling actually impairs FSC self-renewal (Song and Xie, 2003), suggesting that a dynamic pattern of Wnt signaling might be required to maintain the FSC self-renewal program. In addition, fluctuations in Wnt signaling within FSCs might also be important for specifying the fate of the pFCs as they are produced (Dai et al., 2017). It is currently unclear what causes this dynamic pattern of Wnt pathway activation, but one possibility suggested by our finding that Wnt signaling in FSCs is activated by Wg from IGS cells, which undergo continuous rearrangements to facilitate the passage of germ cell cysts through the anterior half of the germarium (Morris and Spradling, 2011), is that the movement of IGS cells influences the amount of Wg ligand available to the FSC niche. This might be important for coordinating FSC niche output with demand from germ cells in the early stages of oogenesis. At the same time, the hierarchy of niche signals we have discovered here could help to ensure that FSC identity is maintained during brief periods of low Wnt signaling. Further studies into the fluctuation of Wnt signaling in relation to other

Development (2018) 145, dev168716. doi:10.1242/dev.168716

signals in FSCs and the movement of IGS cells will continue to provide insights into how this dynamic niche functions.

MATERIALS AND METHODS

Fly stocks

Stocks were maintained on standard molasses food at 25°C and adults were given fresh wet yeast daily. All progeny containing *tub-Gal80^{ts}* were kept at 18°C until eclosion and then shifted to 29°C for 7-10 days for high UAS expression, unless indicated otherwise. The following stocks were used, listed by figure according to the first occurrence (stocks with 'BL' numbers were provided by Bloomington *Drosophila* Stock Center):

Fig. 1: 3×GRH-4TH-EGFP (from Dr Ken Cadigan, University of Michigan, Ann Arbor, MI, USA); w1118; P{GMR13C06-Gal4}attP2 (BL#47860); UAS-wg RNAi (TRiP.HMS00844, BL#33902); FRT82B AxnS044230/TM3 Sb (from Dr Ting Xie, University of Kansas, Lawrence, KS, USA); hsFlp; FRT82B, Ubi-GFP/TM3, Sb (Nystul Laboratory, University of California, San Francisco, CA, USA); and Canton S (BL#64349). Fig. 2: UAS-EGFR RNAi (TRiP.JF01696, BL#31183); UAS-Notch RNAi (TRiP.JF01356, BL#31383); and UAS-EGFR$^{\lambda top}$/TM6C, Sb (BL#59843). Fig. 3: y1, w*; P{GawB}109-30/CyO; (BL#7023) and UAS-HA::wg (BL#5918). Fig. 4: w*; P{GawB}bab1[Pgal4-2]/Tm6b, Tb1 (BL#6803); fz3-RFP (from Dr Ramanuj DasGupta, Genome Institute of Singapore, Singapore); and Nrt::wg [in Wg KO]/CyO; (from Dr Jean Paul Vincent, The Francis Crick Institute, London, UK). Fig. 5: arm^{F} FRT19a/FM7c; (BL#57054); w*, dsh^{3} P{neoFRT}19A/FM7a; (BL#6331); w122 (hsFlp), Ubi-GFP, FRT19a; MKRS/TM3 (from Dr Ben Ohlstein, Columbia University, New York, NY, USA); and UAS-arm RNAi (TRiP.HMS01414, BL#35004). Fig. 6: hsFlp, tsGal80 FRT19a/FM7; Act-Gal4, UAS-CD8 GFP/cyo (Nystul Laboratory) and P{neoFRT}19A; (BL#1709). Fig. 7: P{lacW}spi^{s3547}/cyo; (BL#10462) and UAS-spi RNAi; (BL#34645). Supplementary Figs: UAS-Wnt2 RNAi (TRiP.JF03377, BL#29441); UAS-Wnt4 RNAi (TRiP.JF03378, BL#29442); UAS-Wnt3/5 RNAi (TRiP.HMS0119, BL#34644); UAS-Wnt6 RNAi (TRiP.HM05236, BL#30493); UAS-Wnt8 (TRiP.HM05158, BL#28947); UAS-Wnt10 (TRiP.JF03423, BL#31989); UAS-dsh RNAi (TRiP.JF01253, BL#31306); UAS-dMyc RNAi (TRiPJF01761, BL#25783); Arm^{8}, FRT101/FM7a; (BL#8557); bab1[Agal4-5]/TM3 (sb) (BL#6802); and tsGal80; TM2/TM6 (Nystul Laboratory, University of California, USA).

Immunostaining

Ovaries were dissected in 1× phosphate buffered saline (PBS), fixed in 1× PBS+4% formaldehyde for 15 min, rinsed with 1× PBS+0.2% Triton X-100 (PBST) and blocked for 1 h with 1× PBST containing 0.5% bovine serum albumin (BSA). Samples were incubated with primary antibodies diluted in blocking solution overnight at 4°C. Next, samples were rinsed with PBST and blocked for 1 h before incubating with secondary antibodies for 4 h at room temperature. Samples were rinsed twice with PBST and once with PBS before a final 30 min wash with PBS. For the actin stain in Fig. 1E, Alexa Fluor 488-conjugated phalloidin (Thermo Fisher Scientific, A12379) was added to the last PBS wash at 1:1000 for 30 min, removed, and then the samples were washed a second time with PBS for 30 min. Samples were mounted on glass slides in Vectashield (Vector Laboratories) with 4′,6-diamidino-2-phenylindole (DAPI). For the anti-Wg stain in Fig. S4A, ovaries were dissected in cold 1× PBS and incubated with anti-Wg antibody [1:4; Developmental Studies Hybridoma Bank (DSHB), 4D4], fixed in 1× PBS+4% formaldehyde for 15 min, permeabilized with PBST and blocked for 1 h. Next, samples were incubated with secondary antibody at 1:1000 in block for 4 h at room temperature. Samples were rinsed twice with PBST, blocked for ∼15 min and washed a final time with PBS for 15 min. Samples were mounted on glass slides in Vectashield with DAPI.

The following primary antibodies were used: guinea pig anti-GFP (1:1000; Synaptic Systems, 132005), mouse anti-beta-Galactosidase (1:1000; Promega, Z3781), rabbit anti-Vasa (1:1000; Santa Cruz Biotechnology, sc-30210), mouse anti-Fz2 (1:50; DSHB, 12A7), mouse anti-FasIII (1:50; DSHB, 7G10), rabbit anti-RFP (1:1000; MBL International, PM005S), rat anti-RFP (1:1000; ChromoTek, 5F8), mouse anti-Lamin C (1:100; DSHB, LC28.26), mouse anti-Hts (1:50; DSHB, 1B1) mouse anti-Arm (1:4; DSHB, N27A1), mouse anti-Eya (1:50; DSHB, 10H6); rabbit anti-pERK (1:100; Cell Signaling Technology, 4370), rabbit anti-Castor [1:5000; from Ward Odenwald (Kambadur et al., 1998)], rabbit anti-HA (1:1000; Invitrogen, 71-5500) and mouse anti-EGFR (1:1000; Sigma Aldrich, E2906). The following secondary antibodies were purchased from Thermo Fisher Scientific and used at 1:1000: goat anti-guinea pig 488 (A-11073), goat anti-rabbit 488 (A-11008), goat anti-rabbit 555 (A-21428), goat anti-mouse 488 (A-11029), goat anti-mouse 555 (A-21424) and goat anti-rat 555 (A-21434).

All fixed images were acquired using a Zeiss M2 Axioimager with Apotome unit. For multicolor fluorescence images, each channel was acquired separately. Postacquisition processing, such as image rotation, cropping, and brightness or contrast adjustment, were performed using ImageJ (National Institutes of Health) and Adobe Photoshop. Acquisition settings and any brightness/contrast adjustments were kept constant across conditions within an experiment.

EdU staining

For EdU incorporation experiments, ovaries were dissected and incubated in Schneider's Medium containing 20 µM EdU (Click-it EdU Alexa Fluor 555 Imaging Kit, Life Technologies, C10338) at room temperature for 1 h. Ovaries were then fixed in 4% paraformaldehyde (PFA) for 15 min and washed twice in 1× block (0.5% BSA in PBST). Wash solution was removed and samples were permeabilized with 1× PBST (0.2% Triton X-100 in 1× PBS) for 20 min. Samples were then washed twice with block and then incubated in reaction cocktail (1× Click-iT EdU reaction buffer, $CuSO_4$, Alexa Fluor azide, 1× Click-iT EdU buffer additive) for 30 min at room temperature, protected from light. Finally, tissues were rinsed with 1× PBS and then stained with anti-FasIII primary antibody as described above before mounting on glass slides in Vectashield.

FISH

Flies were fed wet yeast for at least 2 days prior to dissection. The following protocol was performed in RNAse-free conditions. At least 10-20 well-fed flies were dissected in cold 1× Ephrussi-Beadle Ringer's solution (EBR) on a chilled glass plate on ice. Muscle sheath was removed and ovarioles separated while keeping the entire ovary intact. Ovaries were moved to sterile RNAse-free tubes containing 4% PFA in PBS and fixed for 1 h at room temperature. After discarding fix, samples were washed in 1× PBS, then in 50% MeOH in PBS, then 100% MeOH. Samples were then stored in 100% MeOH at −20°C.

Dehydrated samples were taken out of the freezer and rinsed with 100% MeOH, washed with 50% MeOH in EtOH for 5 min, then rinsed with 100% EtOH. Leaving about 100 µl EtOH, the EtOH was removed and replaced with 900 µl xylene. Samples were permeabilized with xylene for 1 h at room temperature. Samples were rinsed twice with EtOH, once with 50% MeOH/EtOH and twice with 100% MeOH. Samples were incubated in 50% MeOH/Fix (5% PFA in PBST) for 5 min, rinsed once with Fix solution and then fixed for 1 h at room temperature. Samples were rinsed three times with PBST, washed for 10 min in PBST and then washed for 10 min in 50% PBST with HYB solution (50% vol/vol formamide, 5× saline-sodium citrate, 0.1% vol/vol of 50 µg/ml heparin, 100 µg/ml transfer RNA and 100 µg/ml sheared, boiled salmon sperm DNA). Samples were incubated with 100% HYB solution in a 60°C water bath overnight.

Then, 400 ng RNA probe was diluted into 50 µl HYB. Probes were heated to 83°C for 2-3 min. Tubes were spun down and put on ice for 5 min, after which 50 µl probe was applied to samples and incubated overnight (up to 24 h) at 60°C overnight.

Samples were washed with preheated HYB over the course of 2 h, switching out washing solution at regular intervals. Samples were rocked at room temperature with 50% HYB/PBST for 5 min. Samples were washed with PBST over the course of 1 h, switching out washing solution at regular intervals. Samples were blocked with 1× Roche blocking reagent in PBST for 1 h at room temperature. Samples were then incubated with pre-adsorbed antibody against Dig diluted 1:500 in 1× block at 4°C overnight.

Primary antibody was removed and samples were rinsed twice with PBST. Samples were then washed over the course of 1 h, switching out washing solution at regular intervals. Samples were blocked for 1 h and then incubated with goat anti-sheep 555 secondary antibody diluted 1:500 in

Development (2018) 145, dev168716. doi:10.1242/dev.168716

block for 1.5 h at room temperature away from light. Secondary antibody was removed and samples rinsed twice with PBST. Samples were washed in the dark over the course of 2 h, switching out washing solution at regular intervals. The last couple of washes were done with PBS instead of PBST. Samples were removed from wash, mounted on slides in Vectashield containing DAPI and imaged as for the immunostaining protocol.

The following probes were used (lower-case letters indicate the primers used to amplify the complementary DNA template in the antiparallel direction): *armadillo*, 5′-ggaacgttgcctctctgtgtCTTGGAAGGCGCGCATAAGCAGTCGCACCAGATGGTGGATGGCCCCGTGCTCCCGCAACGGGGCGTGATTGGCCGGACAGAGGGCCAAATTGCGTATGAGTCCAATGACGGCCTTGATCAAGGGCCAGCGTGATGGTGGATGCAATAGCTTTACAATCACCGATAGTCCGTAGTTTAAGCGTACGGCATTCTGGGCCAACTCAGAGTCCACATGACGCGAGGTCAAGTGACGCAGGGCACATACAGCCGGCTCGGTAATCTCTTCGCGATCTCCAGCATTGATAATAGTACGGACGAGGGCGTCCACACCGCCCACCTGACAAACGGTGGCCTTGTTGCGCTGATTGTTGCACGTCAGATTTGAAAGGATACCGGCGGCACAGGTGACCACGTTGACATCGGTCGAGCCCAGAACCTGGACGAGAGATTGGAGCAAAGCTTCAAGGCCCTCCACCTTAGTGGctgcatccgaaagattgcgg-3′; *dishevelled*, 5′-cgtcaattcggattcggtgcCAAAGAGACTGGTCGAGTCCAGATCGCTGGAGAGCACGGATGCCGATTGATATGTGAGCGGTGGCGGCTGCAGCAGCGGATTGCCCATCATCTTCTGGTGATGGAGCACCTGCTGCTGTTGCTGCTGCGCCAGCTGGACAGGCTGCACCTGCTGCTGCTGTTGTTGTTGCTGTTGCTGGTGCTGCTGCTGCTGTTGTTGTTGCTGCTGCTGATGCTGCTGCTGTTGCTGCTGTAGCTTCCTGTTGGTCAGACCCATGCCCAATTCACACTCACTGGTTGGCAGCTCGGAGCAGTTATCTGACTGATTGGTACCATCGGCGGAGACCAGCCAGGACACCACTCGCCCATTGAAGCAGGGCAGTATGGTGGAGTCGTCGGCTATTTCCTCTTTGACCACACCGAAATCGGCGTCCATTGACTTGAAGAAGTACTTGTAGTTGTTGTTCTGCTTGTTCAGCACCAGCTTGAAATCGCGCAGCGTCACCTGGGCGGATGGAATGGGGATCTTCACCAGATACGGCGTCGTCTCATCGTCGATGTGGTATATCACCTTCGTCTCCTGCCCGCCGCCCCTGTCCGCGTCCATTTTAGCTGCGCCGACTGCGGAAATCCACGGGAAAACTCCTCGACGCGATAAAACGCGATCAAaacgaaatgcgatggatgcg-3′; *frizzled 2*, 5′-gcgggtagtgtttccttccaGACACAGCGCAGCGTCAAATCGTCAACGCTCGACAAACGGCGTGGTCTAACATTTTTTCCATTCCGTTGGCTTTGCTGCTATCTGGTTGATTTTCTGGTTCATTCGATTCCGCCCAGCTGGGGAGCTGGTCCAACTTTCCGCCGTTAATCCCGAAAACTCTTTGGTGGTAATTAAAAAACGCCGTGCGTCTGTCAAAGTTAATCCAATTTCACGTCTGCTTACATCAAACACTCACACTGGCGCACGAACACCTGGAGATGCAGGCACACACGGATACAGCAAGTATCTGACGGATACACAGACACACATATAAATACGTGCGCCGGTTCTTATAGAAACTTTTTGCCGCTGCAAGTAATTTCTACTTTATTTTCGGACAGATTTTTTAATTAATATTTCATGTAGCGCCAAATGTTGTCGCTATCTTTCAGGTGCTACGGTGTGGGATGCTTGTTTTCCTACAGATATATTTAAAGGTGAGCCCCGAGCCCCGAAAATCCAATTTCAGTTGACGCTTGTCGATCAGCGATCACAGATCGGAATAGCAACAATAACAACGAACAGCAAATCTTGTTTCTTTATAACAATTTCCAACACACATTCTCACATGGCACGGCCACAATTTGTATTTTCATAACTCGTTTTCTGTATTTTCTGTCGCTTTTTCGAGGACGCCACTCTACGGTGTTAGCTTGAAGAAACTTCTTTTATTCACGAATGCTTACGATTGATTGTCACtgctttcgatttgcgcacaa-3′; *spitz* (antisense), 5′-atagttcgctccgctcacagCTTGTTGCTGCGTCGAATGGCGAAGGACATTAGCGCGTGCTCCAGCCGCATGTGGTAGGGTAGCTTGCGCTCCAGAATGACTGGCTCCTGGCCATCTGGACAGCACCGGTTGCGGCAGCACTCGCACTGGCCGTCGTCATCGTCGTATTCCTGCTGCAGTTCCTGCTCCAGTTCGTAGGCCTTCTTGGCAGCCCGCTGCTCgaagcgcaaatagaaggcc-3′; *spitz* (sense), 5′-ggccttctatttgcgcttcgAGCAGCGGGCTGCCAAGAAGGCCTACGAACTGGAGCAGGAACTGCAGCAGGAATACGACGATGACGACGGCCAGTGCGAGTGCTGCCGCAACCGGTGCTGTCCAGATGGCCAGGAGCCAGTCATTCTGGAGCGCAAGCTACCCTACCACATGCGGCTGGAGCACGCGCTAATGTCCTTCGCCATTCGACGCAGCAACAAGctgtgagcggagcgaactat-3′.

Clone induction

Flies of the appropriate genotype were cultured and collected upon eclosion. Heat shock was performed by transferring flies to empty plastic vials and immersing them in a 37°C water bath for 1 h. Flies were then allowed to recover at 25°C in vials containing food for at least 5 h. This process was repeated 2× daily for 2 days for a total of 4×1 h heat shocks. Flies were then maintained at 25°C and fed wet yeast daily until dissection.

FSC competition assay

MARCM clones of various genotypes were induced and the frequency of fully labeled, mosaic or no labeled germaria was measured at 7, 14 or 21 days after clone induction. Stem cell labeling counts were analyzed as described previously (Kronen et al., 2014). Replacement events can be measured within the subset of mosaic germaria at the first time point. Over time, mosaic germaria can become unlabeled or fully labeled, indicating replacement. An increase in the proportion of fully labeled germaria is related to the rate of clone expansion, whereas an increase in the proportion of unlabeled germaria is related to the rate of clone extinction. In wild-type tissue, the rates of extinction and expansion are equal. Homozygosity for a mutation that impairs FSC retention in the niche or self-renewal will cause the rate of clone extinction to be higher than the rate of clone expansion.

Statistics

Statistics were performed using Microsoft Excel or R Studio. *N* numbers are provided in the figure legends. *P*-values for figures are as follows (R script and data are provided in the Supplementary Data): Fig. 5: (D) Control versus arm^{8}, $P=3.41\times10^{-4}$; control versus dsh^{3}, $P=1.91\times10^{-3}$; control versus $axn^{S044230}$, $P=0.356$; (F) $P=0.021$. Fig. 6: (B) Control all time points versus dsh^{3} all time points, 2.68×10^{-30}; dsh^{3} all time points versus dsh^{3} with $Egfr^{Jtop}$ all time points, 4.51×10^{-7}; control 7 days after heat shock (dphs) versus dsh^{3} 7 dphs, 2.69×10^{-11}; control 14 dphs versus dsh^{3} 14 dphs, 4.88×10^{-14}; control 21 dphs versus dsh^{3} 21 dphs, 3.03×10^{-11}; dsh^{3} 7 dphs versus dsh^{3} with $Egfr^{Jtop}$ 7 dphs, 0.004; dsh^{3} 14 dphs versus dsh^{3} with $Egfr^{Jtop}$ 14 dphs, 0.046; dsh^{3} 21 dphs versus dsh^{3} with $Egfr^{Jtop}$ 21 dphs, 0.022. Fig. 7: (E) $P=0.001$; (F) $P=0.012$. Fig. S4: (C) Control versus UAS-Wg, 13C06-Gal4, $P=0.271$; control versus UAS-Wg, 109-30-Gal4, $P=8.94\times10^{-20}$. Fig. S5: (D) $P=9.82\times10^{-4}$.

Alignments

Alignments of HMG sites in the *spitz* gene were performed using the UCSC Genome Browser and tools available on the website (https://genome.ucsc.edu; Kent, 2002; Kent et al., 2002)

Acknowledgements

We are grateful to the Bloomington *Drosophila* Stock Center, Ken Cadigan, Ting Xie, Jean Paul Vincent, Ben Ohlstein and Ramanuj DasGupta for stocks and reagents. We also thank FlyBase for curating data into a very useful resource and for providing the ChIPseq data we referenced in this study. Lastly, we thank Katja Rust and Sumitra Tatapudy for helpful comments on the manuscript.

Competing interests

The authors declare no competing or financial interests.

Author contributions

Conceptualization: R.P.K.-Y., T.G.N.; Methodology: R.P.K.-Y., T.G.N.; Formal analysis: R.P.K.-Y., T.G.N.; Investigation: R.P.K.-Y., T.G.N.; Resources: T.G.N.; Data curation: R.P.K.-Y., T.G.N.; Writing - original draft: R.P.K.-Y., T.G.N.; Writing - review & editing: R.P.K.-Y., T.G.N.; Visualization: R.P.K.-Y., T.G.N.; Supervision: T.G.N.; Project administration: T.G.N.; Funding acquisition: T.G.N.

Funding

This research was supported by the National Institutes of Health [R01 GM097158 to T.G.N.; T32 GM007810 and T32 HD007263 'Integrated Training in Reproductive Sciences' to R.P.K.-Y.]. Deposited in PMC for release after 12 months.

Supplementary information

Supplementary information available online at
http://dev.biologists.org/lookup/doi/10.1242/dev.168716.supplemental

References

Alexandre, C., Baena-Lopez, A. and Vincent, J.-P. (2014). Patterning and growth control by membrane-tethered Wingless. *Nature* **505**, 180-185.

Castanieto, A., Johnston, M. J. and Nystul, T. G. (2014). EGFR signaling promotes self-renewal through the establishment of cell polarity in Drosophila follicle stem cells. *Elife* **3**, e04437.

Chang, Y.-C., Jang, A. C.-C., Lin, C.-H. and Montell, D. J. (2013). Castor is required for Hedgehog-dependent cell-fate specification and follicle stem cell maintenance in Drosophila oogenesis. *Proc. Natl. Acad. Sci. USA* **110**, E1734-E1742.
Chen, S., Wang, S. and Xie, T. (2011). Restricting self-renewal signals within the stem cell niche: multiple levels of control. *Curr. Opin. Genet. Dev.* **21**, 684-689.
Clevers, H., Loh, K. M. and Nusse, R. (2014). Stem cell signaling. An integral program for tissue renewal and regeneration: Wnt signaling and stem cell control. *Science* **346**, 1248012.
Contrino, S., Smith, R. N., Butano, D., Carr, A., Hu, F., Lyne, R., Rutherford, K., Kalderimis, A., Sullivan, J., Carbon, S. et al. (2012). modMine: flexible access to modENCODE data. *Nucleic Acids Res.* **40**, D1082-D1088.
Cordero, J. B., Stefanatos, R. K., Myant, K., Vidal, M. and Sansom, O. J. (2012). Non-autonomous crosstalk between the Jak/Stat and Egfr pathways mediates Apc1-driven intestinal stem cell hyperplasia in the Drosophila adult midgut. *Development* **139**, 4524-4535.
Dai, W., Peterson, A., Kenney, T., Burrous, H. and Montell, D. J. (2017). Quantitative microscopy of the Drosophila ovary shows multiple niche signals specify progenitor cell fate. *Nat. Commun.* **8**, 1244.
Freeman, M. and Bienz, M. (2001). EGF receptor/Rolled MAP kinase signalling protects cells against activated Armadillo in the Drosophila eye. *EMBO Rep.* **2**, 157-162.
Haelterman, N. A., Jiang, L., Li, Y., Bayat, V., Sandoval, H., Ugur, B., Tan, K. L., Zhang, K., Bei, D., Xiong, B. et al. (2014). Large-scale identification of chemically induced mutations in Drosophila melanogaster. *Genome Res.* **24**, 1707-1718.
Hamada-Kawaguchi, N., Nore, B. F., Kuwada, Y., Smith, C. I. E. and Yamamoto, D. (2014). Btk29A promotes Wnt4 signaling in the niche to terminate germ cell proliferation in Drosophila. *Science* **343**, 294-297.
Hartman, T. R., Zinshteyn, D., Schofield, H. K., Nicolas, E., Okada, A. and O'Reilly, A. M. (2010). Drosophila Boi limits Hedgehog levels to suppress follicle stem cell proliferation. *J. Cell Biol.* **191**, 943-952.
Hing, H. K., Sun, X. and Artavanis-Tsakonas, S. (1994). Modulation of wingless signaling by Notch in Drosophila. *Mech. Dev.* **47**, 261-268.
Hu, T. and Li, C. (2010). Convergence between Wnt-β-catenin and EGFR signaling in cancer. *Mol. Cancer* **9**, 236.
Johnston, M. J., Bar-Cohen, S., Paroush, Z. and Nystul, T. G. (2016). Phosphorylated Groucho delays differentiation in the follicle stem cell lineage by providing a molecular memory of EGFR signaling in the niche. *Development* **143**, 4631-4642.
Kambadur, R., Koizumi, K., Stivers, C., Nagle, J., Poole, S. J. and Odenwald, W. F. (1998). Regulation of POU genes by castor and hunchback establishes layered compartments in the Drosophila CNS. *Genes Dev.* **12**, 246-260.
Kent, W. J. (2002). BLAT–the BLAST-like alignment tool. *Genome Res.* **12**, 656-664.
Kent, W. J., Sugnet, C. W., Furey, T. S., Roskin, K. M., Pringle, T. H., Zahler, A. M. and Haussler, D. (2002). The human genome browser at UCSC. *Genome Res.* **12**, 996-1006.
Kirilly, D., Spana, E. P., Perrimon, N., Padgett, R. W. and Xie, T. (2005). BMP signaling is required for controlling somatic stem cell self-renewal in the Drosophila ovary. *Dev. Cell* **9**, 651-662.
Kronen, M. R., Schoenfelder, K. P., Klein, A. M. and Nystul, T. G. (2014). Basolateral junction proteins regulate competition for the follicle stem cell niche in the Drosophila ovary. *PLoS ONE* **9**, e101085.
Lee, T. and Luo, L. (2001). Mosaic analysis with a repressible cell marker (MARCM) for Drosophila neural development. *Trends Neurosci.* **24**, 251-254.
Li, X., Han, Y. and Xi, R. (2010). Polycomb group genes Psc and Su(z)2 restrict follicle stem cell self-renewal and extrusion by controlling canonical and noncanonical Wnt signaling. *Genes Dev.* **24**, 933-946.
Llimargas, M. (2000). Wingless and its signalling pathway have common and separable functions during tracheal development. *Development* **127**, 4407-4417.
Lopez-Schier, H. and St Johnston, D. (2001). Delta signaling from the germ line controls the proliferation and differentiation of the somatic follicle cells during Drosophila oogenesis. *Genes Dev.* **15**, 1393-1405.
Margolis, J. and Spradling, A. (1995). Identification and behavior of epithelial stem cells in the Drosophila ovary. *Development* **121**, 3797-3807.
Mirabella, R., Franken, C., van der Krogt, G. N. M., Bisseling, T. and Geurts, R. (2004). Use of the fluorescent timer DsRED-E5 as reporter to monitor dynamics of gene activity in plants. *Plant Physiol.* **135**, 1879-1887.
Morris, L. X. and Spradling, A. C. (2011). Long-term live imaging provides new insight into stem cell regulation and germline-soma coordination in the Drosophila ovary. *Development* **138**, 2207-2215.
Nagaraj, R. and Banerjee, U. (2009). Regulation of Notch and Wingless signalling by phyllopod, a transcriptional target of the EGFR pathway. *EMBO J.* **28**, 337-346.
Nystul, T. G. and Spradling, A. (2007). An epithelial niche in the Drosophila ovary undergoes long-range stem cell replacement. *Cell Stem Cell* **1**, 277-285.
Perrimon, N. and Mahowald, A. P. (1987). Multiple functions of segment polarity genes in Drosophila. *Dev. Biol.* **119**, 587-600.
Reilein, A., Melamed, D., Park, K. S., Berg, A., Cimetta, E., Tandon, N., Vunjak-Novakovic, G., Finkelstein, S. and Kalderon, D. (2017). Alternative direct stem cell derivatives defined by stem cell location and graded Wnt signalling. *Nat. Cell Biol.* **19**, 433-444.
Sahai-Hernandez, P. and Nystul, T. G. (2013). A dynamic population of stromal cells contributes to the follicle stem cell niche in the Drosophila ovary. *Development* **140**, 4490-4498.
Sahai-Hernandez, P., Castanieto, A. and Nystul, T. G. (2012). Drosophila models of epithelial stem cells and their niches. *Wiley Interdiscip. Rev. Dev. Biol.* **1**, 447-457.
Song, X. and Xie, T. (2002). DE-cadherin-mediated cell adhesion is essential for maintaining somatic stem cells in the Drosophila ovary. *Proc. Natl. Acad. Sci. USA* **99**, 14813-14818.
Song, X. and Xie, T. (2003). Wingless signaling regulates the maintenance of ovarian somatic stem cells in Drosophila. *Development* **130**, 3259-3268.
Su, T.-Y., Nakato, E., Choi, P. Y. and Nakato, H. (2018). Drosophila glypicans regulate follicle stem cell maintenance and niche competition. *Genetics* **209**, 537-549.
Swarup, S. and Verheyen, E. M. (2012). Wnt/wingless signaling in Drosophila. *Cold Spring Harb. Perspect. Biol.* **4**, a007930-a007930.
Szüts, D., Freeman, M. and Bienz, M. (1997). Antagonism between EGFR and Wingless signalling in the larval cuticle of Drosophila. *Development* **124**, 3209-3219.
Upadhyay, M., Martino Cortez, Y., Wong-Deyrup, S., Tavares, L., Schowalter, S., Flora, P., Hill, C., Nasrallah, M. A., Chittur, S. and Rangan, P. (2016). Transposon dysregulation modulates dwnt4 signaling to control germline stem cell differentiation in Drosophila. *PLoS Genet.* **12**, e1005918.
Upadhyay, M., Kuna, M., Tudor, S., Martino Cortez, Y. and Rangan, P. (2018). A switch in the mode of Wnt signaling orchestrates the formation of germline stem cell differentiation niche in Drosophila. *PLoS Genet.* **14**, e1007154.
van Amerongen, R. and Nusse, R. (2009). Towards an integrated view of Wnt signaling in development. *Development* **136**, 3205-3214.
Wang, X. and Page-McCaw, A. (2014). A matrix metalloproteinase mediates long-distance attenuation of stem cell proliferation. *J. Cell Biol.* **206**, 923-936.
Wang, X. and Page-McCaw, A. (2018). Wnt6 maintains anterior escort cells as an integral component of the germline stem cell niche. *Development* **145**, dev158527.
Wang, S., Gao, Y., Song, X., Ma, X., Zhu, X., Mao, Y., Yang, Z., Ni, J., Li, H., Malanowski, K. E. et al. (2015). Wnt signaling-mediated redox regulation maintains the germ line stem cell differentiation niche. *Elife* **4**, e08174.
Wasserman, J. D. and Freeman, M. (1998). An autoregulatory cascade of EGF receptor signaling patterns the Drosophila egg. *Cell* **95**, 355-364.
Yamamoto, S., Jaiswal, M., Charng, W.-L., Gambin, T., Karaca, E., Mirzaa, G., Wiszniewski, W., Sandoval, H., Haelterman, N. A., Xiong, B. et al. (2014). A drosophila genetic resource of mutants to study mechanisms underlying human genetic diseases. *Cell* **159**, 200-214.
Zhang, C. U., Blauwkamp, T. A., Burby, P. E. and Cadigan, K. M. (2014). Wnt-mediated repression via bipartite DNA recognition by TCF in the Drosophila hematopoietic system. *PLoS Genet.* **10**, e1004509.

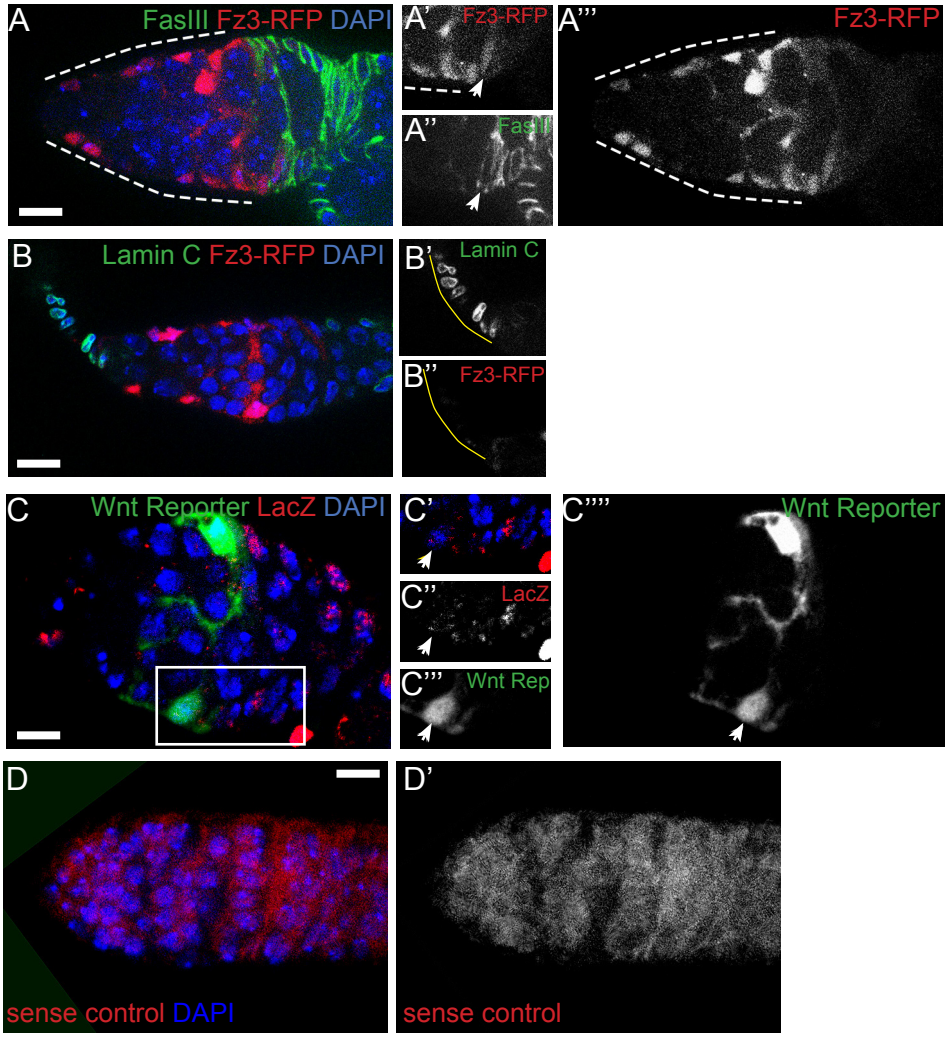

Figure S1: (A) A germarium with the *Fz3-RFP* Wnt reporter stained for RFP (red), FasIII (green), and DAPI (blue). The RFP and FasIII channels are shown separately for the region surrounding the anterior-most FasIII^{+} cell (white arrow) in A' and A" and the RFP channel for the full image is shown in A"'. RFP expression is detectable in IGS cells in Regions 1 and 2a (white dashed lines) and in FSCs (white arrow in A' and A"), identified as the anterior-most FasIII^{+} cells (A"), but expression rapidly decreases in pFCs downstream from the niche. (B) A germarium with *Fz3-RFP* stained for RFP (red), Lamin C (green) to mark the cap and terminal filament cells, and DAPI (C). *Fz3-RFP* is not detectable in Lamin C^{+} cells (solid yellow line). (C) A germarium with the *3xGRH-4TH-GFP* reporter and a LacZ negatively marked clonal marking system to identify FSCs stained for LacZ (clone marker, red), GFP (green), and DAPI (blue). FSCs are marked as the anterior-most cell in a LacZ negative clone (C', C" arrow). *3xGRH-4TH-GFP* is detectable in FSCs (C"', C"" arrow) but not pFCs downstream. (D) A negative control for all FISH experiments in Figure 1. The probe matches the *spitz* sense strand sequence. Scale bar represents 5 μm.

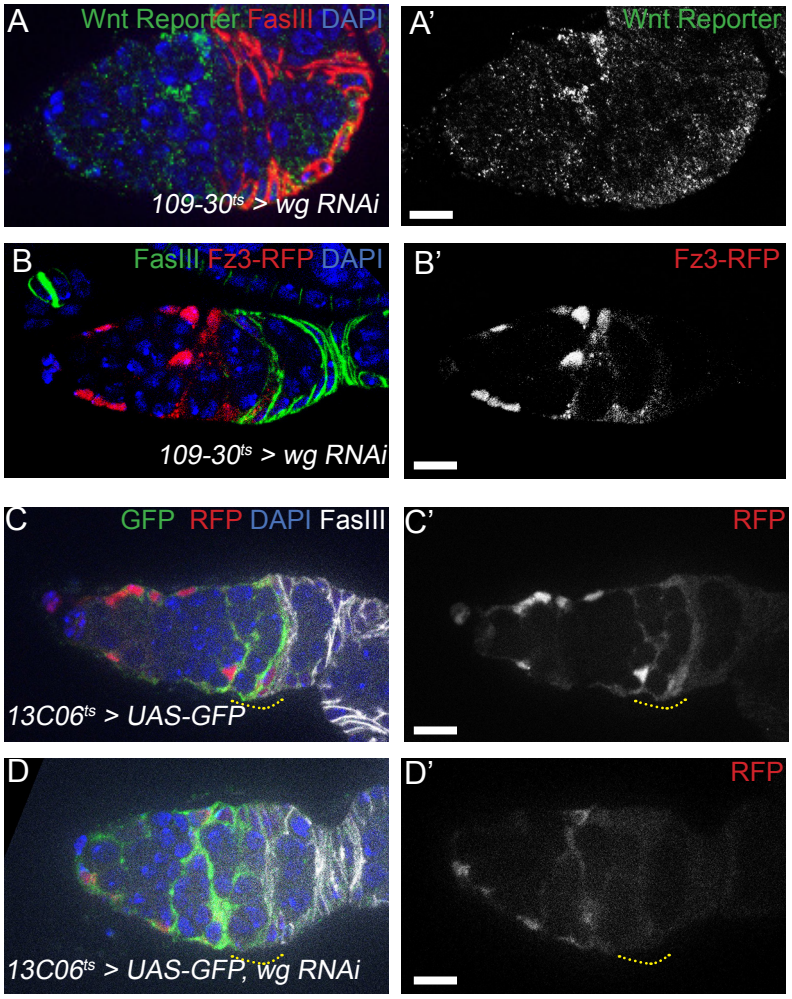

Figure S2: (A-B) The *3xGRH-4TH-GFP* reporter (A) or the *Fz3-RFP* reporter (B) combined with *UAS-wg RNAi*, *109-30-Gal4*, and *tub-Gal80^{ts}* to restrict expression to adulthood stained for GFP (green in A) or RFP (red in B), FasIII (red in A, green in B), and DAPI (blue). Wg knockdown with this driver reduces but does not eliminate *3xGRH-4TH-GFP* expression, and does not affect *Fz3-RFP* expression. (C-D) Germaria with either *13C06-Gal4* driving *CD8-GFP* as a control (C) or *13C06-Gal4* driving *CD8-GFP* and *wg* RNAi (D) stained for FasIII (white), GFP (green), RFP (red), and DAPI (blue). In germaria with *wg* RNAi expressed using *13C06-Gal4*, RFP expression is reduced overall and undetectable in the posterior region of *13C06-Gal4* expression domain (dotted yellow line), which includes FSCs, identified as the anterior most FasIII^{+} cells, and posterior IGS cells. Scale bar represents 5 μm.

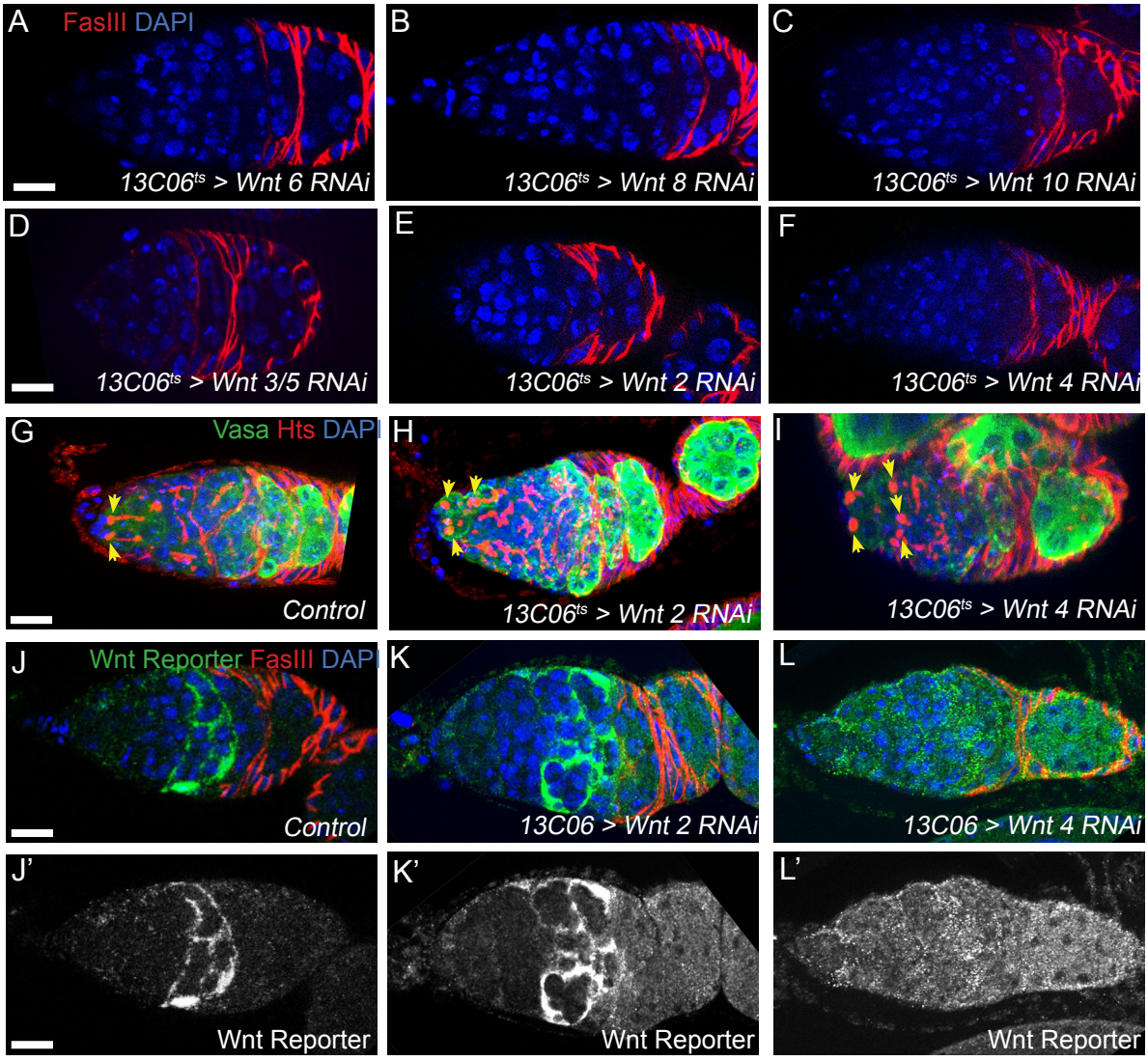

Figure S3: (A-F) Germaria with RNAi against *Wnt6* (A), *Wnt8* (B), *Wnt10* (C), *Wnt3/5* (D), *Wnt2* (E) or *Wnt4* (F) driven with *13C06-Gal4* and combined with *tub-Gal80^{ts}* to restrict expression to adulthood stained for FasIII (red) and DAPI (blue). No significant morphological phenotypes, as visualized with FasIII staining, were observed. (G-H) Maximum intensity projections of 5-10 optical sections of wildtype control (G), *Wnt2* RNAi (H), or *Wnt4* RNAi (I) stained for Hts (red) to identify spectrosomes (yellow arrows), vasa (green) and DAPI (blue). *Wnt2* and *Wnt4* knockdown exhibit more spectrosomes compared to control. (J-L) Germaria with *3xGRH-4TH-GFP*, *13C06-Gal4*, and either no RNAi as a control (J), *Wnt2* RNAi (K), or *Wnt4* RNAi (L) stained for FasIII (red), GFP (green), and DAPI (blue). Expression of *Wnt2* RNAi had no effect on *3xGRH-4TH-GFP* reporter levels whereas expression of *Wnt4* RNAi caused in a reduction in the *3xGRH-4TH-GFP* reporter levels. The GFP channels are shown in J'-L'. Scale bar represents 5 μm.

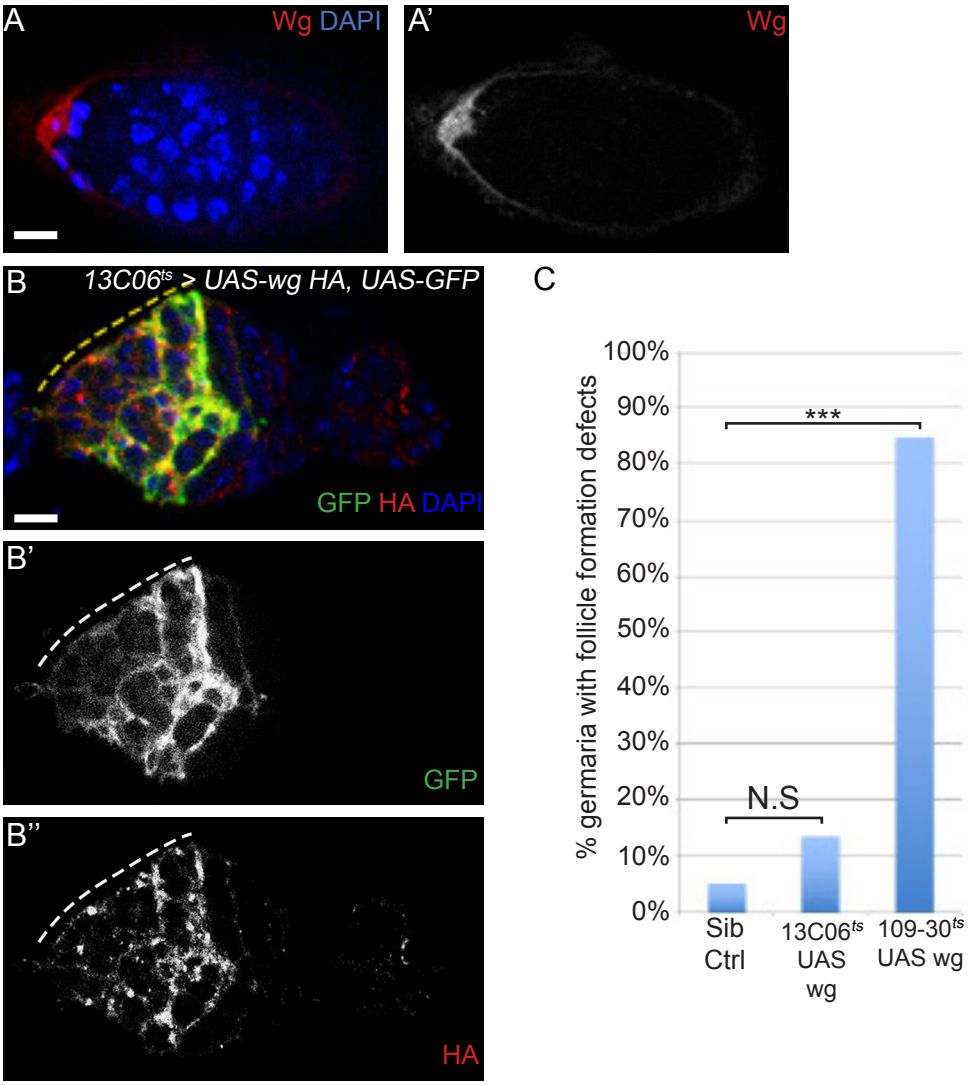

Figure S4: (A) A wildtype germarium stained for Wg (red) and DAPI (blue). The Wg signal is strongest at the anterior tip of the germarium, and tapers off toward the posterior in Regions 1 and 2a. The Wg channel is shown separately in A'. (B) Panels showing the merged image (B), GFP only channel (B'), and HA::Wg channel (B") from the image in Figure 3D. The HA::Wg signal overlaps precisely with the GFP signal (dotted lines) (C) Quantification of follicle formation defects in flies with *tub-Gal80^{ts}*, *UAS-HA::Wg*, and either *13C06-Gal4*, *109-30-Gal4*, or CyO siblings that lack a Gal4 driver shifted to 29°C for 7 days during adulthood to inactivate Gal80 and allow for *HA::Wg* expression. ***p<0.001 and N.S. indicates not significant with a chi-squared test. n>50 germaria. Scale bar represents 5 μm.

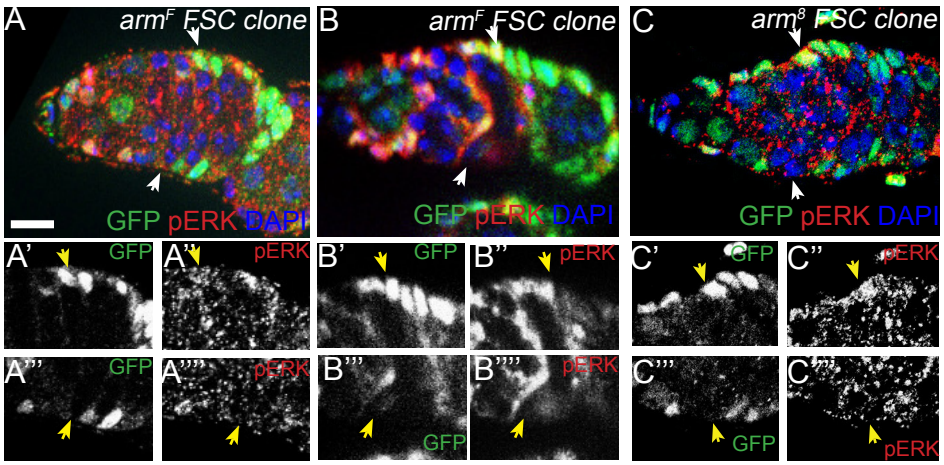

D

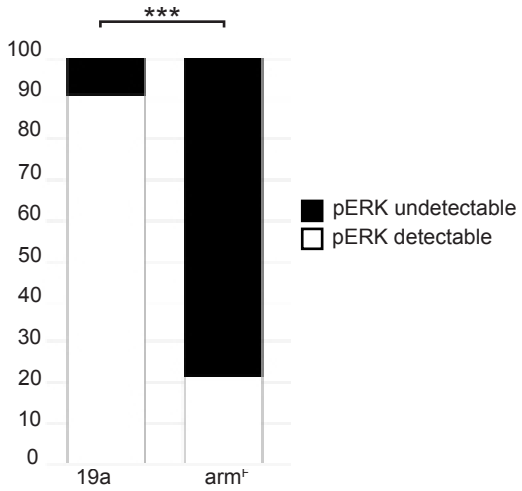

E

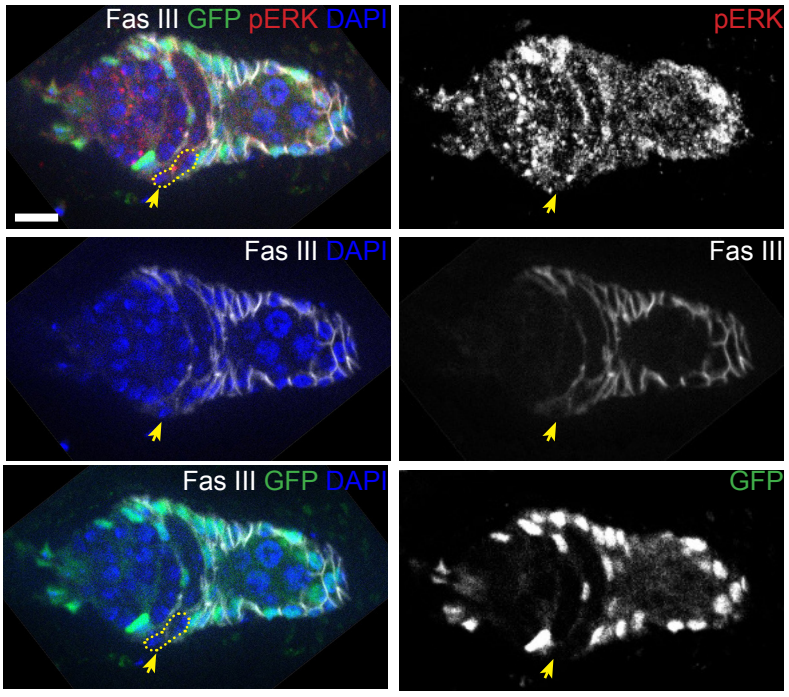

Figure S5: (A-C) Germaria with *arm*^{F} (A-B) or *arm*^{8} (C) clones stained for pERK (red), GFP (clonal marker, green) and DAPI (blue). Images are oriented with a GFP^{+} (wildtype) FSC on top and a GFP^{-} (homozygous mutant) FSC on the bottom. FSCs (arrows) are identified as the anterior-most cell in an FSC clone and by their position at the Region 2a/2b border. Wildtype control FSCs are pERK^{+} in each case whereas *arm*^{F} and *arm*^{8} FSCs are pERK^{-}. (D) Quantification of germaria with pERK^{+} GFP^{-} FSCs in germaria in which the wildtype (GFP^{+}) FSC is pERK^{+} for the indicated genotypes. ***P<0.001 using a two-sided Fisher Exact test. (E) A demonstration of the criteria used to identify FSCs using the image of the germarium with a *dsh*^{3} mutant clone shown in Figure 5B. FasIII is white, GFP is green, pERK is red, DAPI is blue, and the FasIII, GFP, and pERK channels are shown separately. FSCs are identified by scrolling through the optical sections to find the anterior-most marked cell (GFP^{-}) in a clone. Because this cell also the anterior-most FasIII^{+} cell, we used the border of FasIII staining to identify the FSCs in other cases when a clone is not present. The FSC is indicated with a yellow arrow and the GFP^{-} clone is outlined with a yellow dotted line. Scale bar represents 5 μm.

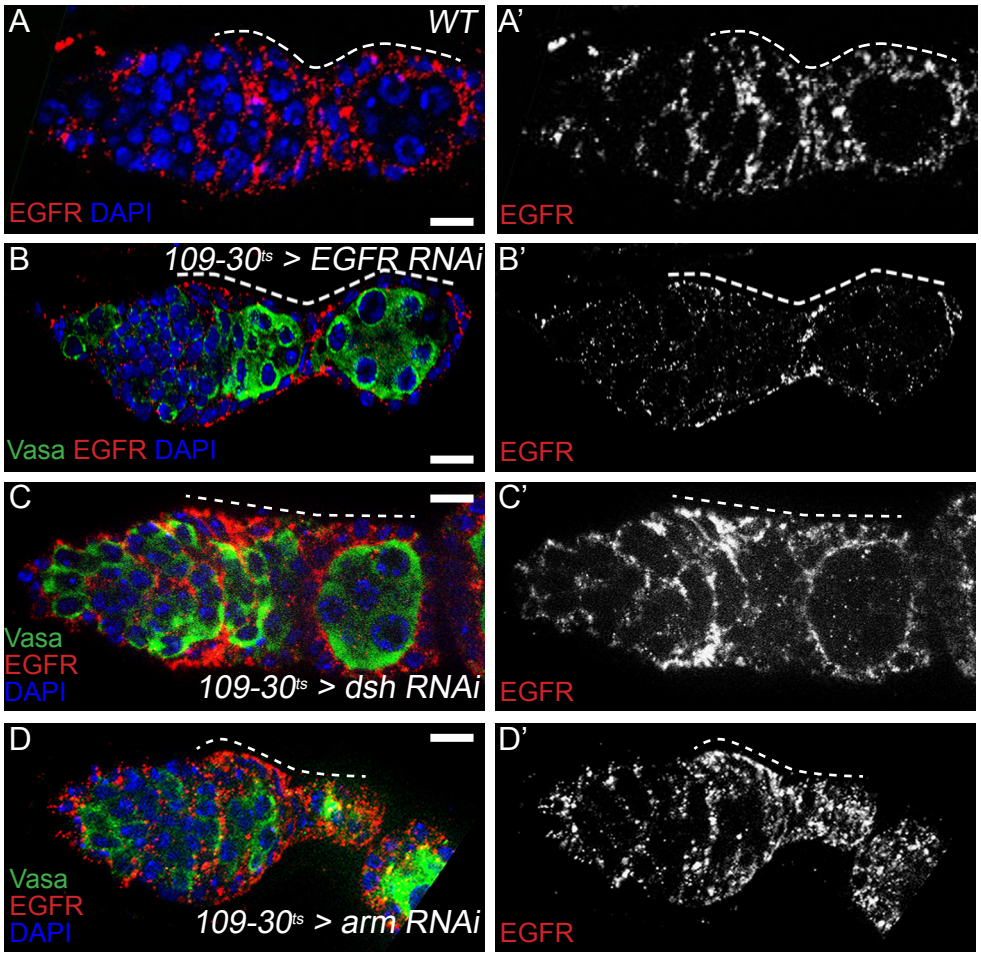

Figure S6: (A-D) A wildtype germarium (A) or germarium with *UAS-EGFR RNAi* (B), *UAS- dsh* RNAi (C), or *UAS-arm* RNAi (D) combined with *109-30-Gal4* and *tub-Gal80^{ts}* to restrict expression to adulthood (B) stained for EGFR (red), vasa (panels B-D, green) and DAPI (blue). EGFR expression is detectable in FSCs and pFCs (dotted lines) of wildtype germaria and is unaffected by expression of *dsh* RNAi or *arm* RNAi, but is substantially reduced by expression of *EGFR* RNAi. Scale bar represents 5 μm.

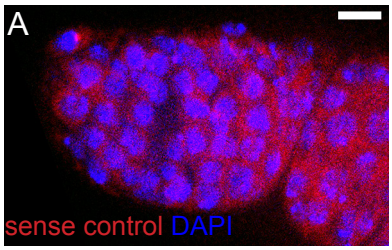

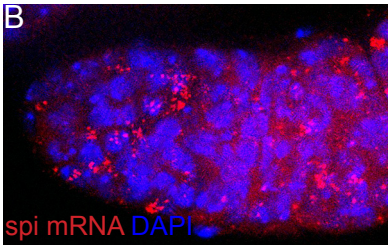

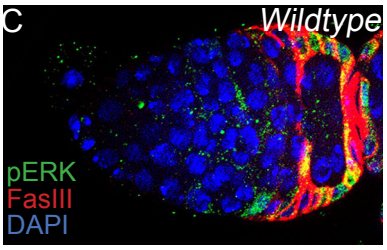

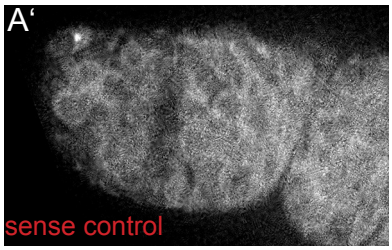

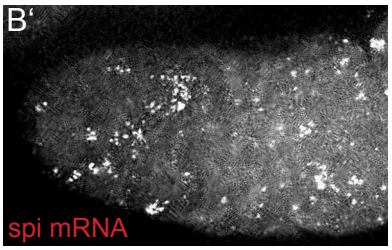

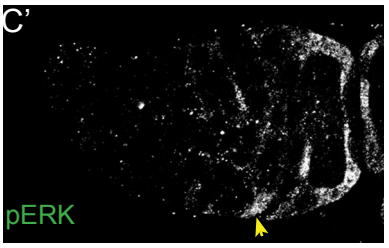

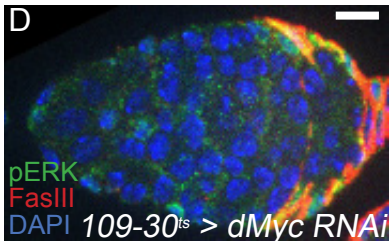

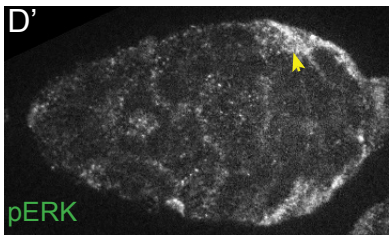

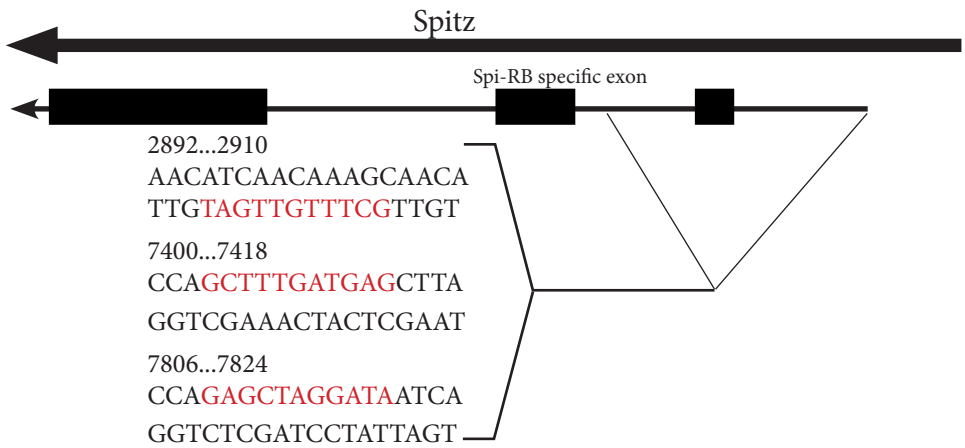

F

```
D. mel. chrII coords. 19574403|                                  19574445|
D. melanogaster              gttctgttgc-tttgttgatgttacaattgttgcacttgttg
D. simulans                  gttctgttgc-tttgttgatgttacaattgttgcacttgttg
D. sechellia                 gttttgttgc-tttgttgatgttacaattgttgcacttgttg
D. yakuba                    gttctgttgc-tttgttgatgttacaattgttgcacttgttg
D. erecta                    gttcggttgc-tttgttgatgttacaattgttgcacttgttg
D. biarmipes                 gctctgttcctttgttgatgttacaattgttgcacttgttg
D. suzukii                   gttctgttcctttgttgatgttacaattgttgcacttgttg
D. ananassae                 -----gttgc-tt----------caattgttgcacttgttg
D. bipectinata               -----gttgc-tt----------caattgttgcacttgttg
D. eugracilis                gttctgttgctttgttgatgttacaattgttgcacttgttg
D. elegans                   gttctgttgctttgttgatgttacaattgttgcacttgttg
D. kikkawai                  gttctgttgctgtttttgatgctacaattgttgcacttgttg
D. takahashii                gttctgttgctttgttgatgttacaattgttgcacttgttg
D. rhopaloa                  gttctgttgctttgttgatgttacaattgttgcacttgttg
D. ficusphila                gttctgttgctttgttgatgttacaa-tgttgcacttgttg
D. willistoni                cttccattcc----------ctacaattgttgcacttgttg
D. grimshawi                 gcattgctta-ctagttgttattattgttgttgcacttgttg
A. gambiae                   gttctgcttgttcgtttaataatattactatattaattattg

D. mel. chrII coords. 19569905|                          19569932|
D. melanogaster              ctaagctcatcaaagctggctgtgata
D. simulans                  ctaagctcatcaaagctggctgtgata
D. sechellia                 ctaagctcatcaaagctggctgtgata
D. yakuba                    ctaagctcatcaaagctggctgtgata
D. erecta                    ctaagctcatcaaagctggctgtgata
D. biarmipes                 ctaagctcatcaaagctggctgtgata
D. suzukii                   ctaagctcatcaaagctggctgtgata
D. ananassae                 ctaagctcatcaaagctggctgtgata
D. bipectinata               ctaagctcatcaaagctggctgtgata
D. eugracilis                ctaagctcatcaaagctggctgtgata
D. elegans                   ctaagctcatcaaagctggctgtgata
D. kikkawai                  ctaagctcatcaaagctggctgtgata
D. takahashii                ctaagctcatcaaagctggctgtgata
D. rhopaloa                  ctaagctcatcaaagctggctgtgata
D. ficusphila                ctaagctcatcaaagctggctgtgata
D. willistoni                cagagctcatcaaagctggctgtgata
D. virilis                   ctaagctcatcaaagctggctgtgata
D. mojavensis                ctaagctcatcaaagctggctgtgata
D. albomicans                ctaagctcatcaaagctggctgtgata
D. grimshawi                 ctaagctcatcaaagctggctgtgata
M. domestica                 ctcagctcatcaaagctggctgtgata
A. gambiae                   cctagctcatcaaagctggctgtgata
A. mellifera                 ccacgctcatcaaagctggctgtgata
T. castaneum                 ctgtgctcatcaaagctggctgtgata

D. mel. chrII coords. 19569499|                                  19569527|
D. melanogaster              gctcatcaaagctggctgtgatatgcgt
D. simulans                  gctcatcaaagctggctgtgatatgcgt
D. sechellia                 gctcatcaaagctggctgtgatatgcgt
D. yakuba                    gctcatcaaagctggctgtgatatgcgt
D. erecta                    gctcatcaaagctggctgtgatatgcgt
D. biarmipes                 gctcatcaaagctggctgtgatatgcgt
D. suzukii                   gctcatcaaagctggctgtgatatgcgt
D. ananassae                 gctcatcaaagctggctgtgatatgcgt
D. bipectinata               gctcatcaaagctggctgtgatatgcgt
D. eugracilis                gctcatcaaagctggctgtgatatgcgt
D. elegans                   gctcatcaaagctggctgtgatatgcgt
D. kikkawai                  gctcatcaaagctggctgtgatatgcgt
D. takahashii                gctcatcaaagctggctgtgatatgcgt
D. rhopaloa                  gctcatcaaagctggctgtgatatgcgt
D. ficusphila                gctcatcaaagctggctgtgatatgcgt
D. willistoni                gctcatcaaagctggctgtgatatgcgt
D. virilis                   gctcatcaaagctggctgtgatatgcgt
D. mojavensis                gctcatcaaagctggctgtgatatgcgt
D. albomicans                gctcatcaaagctggctgtgatatgcgt
D. grimshawi                 gctcatcaaagctggctgtgatatgcgt
M. domestica                 gctcatcaaagctggctgtgatatgcgt
A. mellifera                 gctcatcaaagctggctgtgatacgagt
T. castaneum                 gctcatcaaagctggctgtgatatgagc
```

Figure S7: (A-B) Wildtype germaria incubated with a FISH probe (red) that matches either the *spitz* sense strand as a negative control (A) or the *spitz* anti-sense strand to detect *spitz* transcript (B) and stained with DAPI (blue). (C-D) A wildtype (Canton-S) germarium or germarium with *dMyc* RNAi driven with *109-30-Gal4* and with *tub-Gal80^{ts}* to restrict expression to adulthood stained for FasIII (red), pERK (green), and DAPI (blue). *dMyc* knockdown does not eliminate the pERK signal in FSCs (yellow arrow), identified as the anterior most FasIII^{+} cells. Scale bar represents 5 μm. (E) Putative TCF binding sites in the TSS of two *spitz* isoforms: Spi-RB and Spi-RE. Predicted High Mobility Group (HMG) recognition motifs are highlighted in red. (F) Alignments of HMG binding sites shown in (E) throughout multiple dipteran insect 75 species performed using the UCSC genome browser. Conserved sequences are highlighted in yellow.

Supplementary Data Files: The raw data for all of the quantifications reported in the paper (Figures 5, 6, 7, S4, and S5) are included as an Rdata file. The statistical analyses of these data are provided as an Rmd file and an HTML file. The Rdata file and Rmd file can be opened in RStudio (www.rstudio.com) and the HTML file can be opened in standard web browsers.

Click here to download HTML Data file

Click here to download Rmd Data file

Click here to download Rdata Data file